

**On Training Implicit
Meta-Learning With Applications
to Inductive Weighing in
Consistency Regularization**

Fady Rezk

Master of Science
Informatics
School of Informatics
University of Edinburgh
2021

Abstract

Meta-learning that uses implicit gradient have provided an exciting alternative to standard techniques which depend on the trajectory of the inner loop training. Implicit meta-learning (IML), however, require computing 2^{nd} order gradients, particularly the Hessian which is impractical to compute for modern deep learning models. Various approximations for the Hessian were proposed but a systematic comparison of their compute cost, stability, generalization of solution found and estimation accuracy were largely overlooked. In this study, we start by conducting a systematic comparative analysis of the various approximation methods and their effect when incorporated into IML training routines. We establish situations where catastrophic forgetting is exhibited in IML and explain their cause in terms of the inability of the approximations to estimate the curvature at convergence points. Sources of IML training instability are demonstrated and remedied. A detailed analysis of the efficiency of various inverse Hessian-vector product approximation methods is also provided. Subsequently, we use the insights gained to propose and evaluate a novel semi-supervised learning algorithm that learns to inductively weigh consistency regularization losses. We show how training a “Confidence Network” to extract domain specific features can learn to up-weight useful images and down-weight out-of-distribution samples. Results outperform the baseline FixMatch performance.

Acknowledgements

I would like to thank my supervisor, Professor Timothy Hospedales, for proposing and supervising this intriguing project. Your generosity with your time for supporting and mentoring me throughout the project was a great source of encouragement and learning. Your thought provoking questions that were asked at the perfect time have developed my skills and critical thinking as an aspiring researcher and I am grateful for that.

My sincere gratitude also goes to Dr. Ondrej Bohdal, my co-supervisor. Your prompt replies to my questions, making the time to meet me on short-notice even late in the evenings and spending generous amount of time discussing avenues of investigations was deeply appreciated. Whenever I lost focus or deviated from the main goals of my research, you have always helped me redirect my attention. In times of disorientation, your guidance fixated my focus again.

Professor Hospedales and Ondrej, your kindness when meetings ran over and generosity with your times to push this project to the current standard is deeply appreciated. Thanks for the great learning opportunity.

I would also like to thank Dr. Antreas Antoniou. Our discussions have always been a space of growing for me where I learnt to better read, critically evaluate and question research literature. Your readiness to always help and commitment to teaching has supported me throughout my Master's.

I would like to both thank and congratulate my close friend, Dr. Mohamed ElGhazaly, who only 2 days ago passed his PhD viva. Your check up calls have always been a wonderful source of support at times of stress. Your supportive and motivating words always helped me push myself. Our Pomodoro meetings were the funniest and most efficient study sessions I ever been in.

Many thanks for the generous support of Ahmed Ramy, CEO and founder of both TMentors Cairo and FastAutomate, for providing the GPU and compute resources used to run this dissertation's experiments.

Last but not least, I want to send out my gratitude and love to my family for their unwavering support during my whole Master's. Your support at times of stress and encouraging words were always heartwarming.

Declaration

I declare that this thesis was composed by myself, that the work contained herein is my own except where explicitly stated otherwise in the text, and that this work has not been submitted for any other degree or professional qualification except as specified.

(Fady Rezk)

Table of Contents

1	Introduction	1
1.1	Motivation	1
1.2	Goals	2
1.3	Contributions	3
1.4	Report Outline	4
2	Background	5
2.1	Meta-Learning Overview	5
2.2	Semi-Supervised Learning	6
2.2.1	Overview	6
2.2.2	FixMatch	7
2.3	Meta-Learning for SSL	8
2.4	Critique	9
3	Implicit Meta-Learning	10
3.1	Overview	10
3.2	Approximating Inverse Hessians	12
3.2.1	Neumann Series	12
3.2.2	Conjugate Gradient	13
3.2.3	Identity Matrix For IML vs T1-T2	13
3.2.4	Note	14
3.3	Proposed Methodology	14
4	Experiments and Results	16
4.1	Learning Per Parameter Regularizer	16
4.1.1	Training Details	16
4.1.2	Overfitting a Small Validation Set Results	16

4.1.3	Approximation Methods Comparison to Exact Inverse Hessian-Vector Product	19
4.1.4	Compute Cost	21
4.2	Learning Per Layer Regularizer	24
4.2.1	Training Details	24
4.2.2	Generalization Power	25
4.2.3	Compute Cost	27
4.2.4	Ablation Study	27
4.3	Discussion	29
4.3.1	Summary	29
4.3.2	Critique and Future Work	30
5	Confidence Network for FixMatch	31
5.1	Introduction	31
5.2	Algorithm	32
5.3	Evaluation and Results	33
5.3.1	Training Details	33
5.3.2	Results	35
5.4	What did the model learn?	36
5.5	Conclusion and Further Work	38
6	Conclusion	39
6.1	Summary and Reflection	39
6.2	Future Work	40
	Bibliography	41
A	Overfitting a Small Validation Set	46
A.1	Detailed Experiment Results	46
A.2	Baselines Regularization Results	51
A.3	Training Evolution Plots for Main Experiments	52
B	Ablation Study Training Evolution Plots	56

Chapter 1

Introduction

1.1 Motivation

With the advent of the internet and the ubiquity of data collection pipelines, enormous amounts of data have been and are being continuously curated, labeled, and annotated. Models trained on these datasets are considered “intelligent” as they execute a variety of tasks after learning embedded patterns in the data, including but not limited to making predictions on new data as they arrive. Deep Learning [1] has achieved remarkable performance in a wide variety of tasks such as image recognition [2, 3], natural language processing [4] and speech recognition [5] among others.

Deep Learning, nonetheless, faces two major limitations. First, all deep learning algorithms require expensive hyperparameters optimization for improving performance. Secondly, deep learning models require a tremendous amount of labeled data to learn. With the time and monetary costs associated with manually annotating data especially in expert domains such as in medical research, it is paramount to capitalize on the availability of large unlabelled sets that might contain out-of-domain samples.

Semi-Supervised Learning (SSL) addresses the later limitation. Previous SSL approaches have achieved comparable and competitive results to supervised algorithms which train on a large scale labeled data [6–9]. However, SSL algorithms introduce more hyperparameters to benefit from the unlabelled data. Additionally, it treats all unlabelled data as equally beneficial and attempting to disregard out-of-domain samples is as strenuous and laborious as labeling them.

Meta-Learning (or learning to learn) [10] paradigm allows to learn such meta-knowledge using same available data [11] or with the cost of needing an extra small labelled dataset [12]. Meta-Knowledge includes, but is not limited to, hyperparameters

which address the first limitation of training Deep Learning models. Put simply, the meta-learning paradigm attempts to learn some knowledge about the learning process itself. The review [10] introduces a meta-learning taxonomy: Meta-Representation (what am I learning about the learning process?), Meta-Optimizer (How is this knowledge learned?) and Meta-Objective (Why is this knowledge learned?). The most famous Meta-Optimizers are gradient descent variants. MAML [13] is the most famous technique and by design is agnostic of the inner-loop task and model. Therefore, the method is easily applicable to any base model of choice and task which we aim to learn some meta-knowledge for.

Meta-Learning, however, requires tremendous memory and time resources. Therefore, gradient-based approaches such as MAML have focused on few-shot regimes. Recent research efforts have been oriented towards scaling Meta-Learning to many-shot regimes. Most famously, Implicit Meta-Learning (IML) [14] trains base model till convergence which allows using Implicit Function Theorem (IFT) to bypass unrolled differentiation and only backpropagates through the last step. It also claims to scale to millions of hyperparameters without placing extra strain on computational resources needed although using IFT introduces the requirement of computing second-order gradients and hence the need to provide estimates for the Hessian. The method offers an exciting alternative of another avenue of research since being able to use more inner-loop steps usually translates to finding better solutions in practice.

1.2 Goals

The concerns of this research project are two-fold. First, it is unclear how inverse hessian-vector product approximations, such as Neumann Series [14], Conjugate Gradient or Identity Matrix approximation [15], used in IML compare to the exact inverse Hessian. Previous studies have not scrutinized when these methods succeed, fail or when to choose one over the other. Training the inner-loop till convergence is usually ignored in practice and IML is used in semi-online settings (taking many inner steps without reaching convergence before a meta-update) without investigating how this influences the performance of overall solutions. In addition, there is a knowledge gap in the research literature for systematically studying the costs of respective approximations or systematically juxtaposing the performance of solutions found by each method. Therefore, the first part of the study introduces a comparative analysis of different inverse Hessian approximation techniques and their influence on the accu-

racy of the solution found, memory consumption, compute cost, comparison to exact inverse hessian, and their respective stability. Additionally, the convergence assumption is revisited.

Subsequently, insights are used to design a novel inductive semi-supervised algorithm that learns to weigh unlabelled data points in a meta-learning setting. Our algorithm learns to learn prioritizing unlabelled images. To maximize base model performance, it learns to down-weigh out-of-domain samples and emphasizes relevant ones. This is achieved through building meta-knowledge regarding which visual features directly contribute to improving semi-supervised algorithm accuracy and loss. This meta-visual feature extractor is denoted Confidence Network. The Confidence Network's learned representation transforms unlabelled images to a weight resembling how *confident* is the network that the unlabelled image would improve the base models' performance.

In summary, the goals of the project are:

1. Investigate Implicit Meta-Learning training, compare inverse Hessian-vector product approximation methods estimation accuracy against exact computation and juxtapose the methods in terms of generalization of the solution found, compute cost, and stability
2. Design and evaluate a novel inductive semi-supervised learning algorithm that exploits the power of Implicit Meta-Learning

1.3 Contributions

The contributions of this study are:

1. Present how catastrophic forgetting phenomenon is exhibited in IML, establish one source/cause of it in terms of approximation method inability to estimate the loss function curvature beyond convergence, and propose a basic solution to it
2. Show and explain the counter-intuitive fact that using more terms/iterations in either Neumann Series or Conjugate Gradient approximations degrades overall approximation power and final solution performance
3. Establish sources of instability in IML, namely under-estimation of training loss at the start of training, and propose a solution that both remedies the issue and cuts down the base model training steps till convergence by half

4. Show the power of IML, if trained correctly, in significantly improving over baselines
5. Provide a detailed evaluation of the efficiency and estimation accuracy of different 2^{nd} order gradient approximation methods employed in implicit meta-learning
6. Propose and evaluate a novel semi-supervised algorithm that outperforms Fix-Match baseline by learning to inductively weigh consistency regularization loss
7. Establish shortcomings of our proposed method and propose future directions to resolve and address them

1.4 Report Outline

In chapter 2, the necessary and required background to understand the dissertation is covered. Relevant literature is reviewed to ground this dissertation's investigations and proposals in previous work. Next, chapter 3 provides a detailed and formal treatment of Implicit Meta-Learning along with the various inverse-Hessian approximation methods employed in the comparative analysis. Subsequently, the experiments conducted, results, findings, and discussions for the first goal of this dissertation are detailed in chapter 4.

The findings and insights of the first part of this dissertation are then used to design a novel Semi-Supervised Learning algorithm. The algorithm, titled Fixing FixMatch, is introduced and derived formally in chapter 5. The training details, preliminary experiments, and initial results are also covered besides a critique of the proposal and directions for further improvement. Finally, chapter 6 concludes the dissertation and summarizes all the work done herein.

Chapter 2

Background

2.1 Meta-Learning Overview

This study focuses on gradient-based Meta-Learning which is the most efficient and widely adopted formulation. For a full review on Meta-Learning, please refer to the most recent survey by *Hospedales et al.* [10]. To introduce Meta-Learning, one has to start with Model Agnostic Meta-Learning (MAML) [13]. MAML, as said earlier, focuses on the few-shot regime and was designed with few-shot learning in mind. It attempts to learn some meta-knowledge such as deep network initialization $\theta = \theta_0$ whose meta-objective is generalizing to new unseen downstream tasks as fast as possible with few labels per class. MAML is a great starting point to introduce Meta-Learning.

Let f_θ be a deep network parameterized by θ . Given a distribution over tasks $p(\mathcal{T})$, MAML samples a task \mathcal{T}_i and trains the base model on it using a support (training) set for few episodes. Subsequently, a query (validation) set is used to evaluate the performance of the base model to update the meta-knowledge. MAML produces new base model parameters θ'_i by taking one or multiple standard gradient-descent steps, i.e: $\theta'_i = \theta - \alpha \nabla_{\theta} \mathcal{L}_{\mathcal{T}_i}(f_\theta)$ where α is the learning rate (can be fixed or meta-learned). Thereafter, the meta-knowledge θ is updated by minimizing the validation loss on the query set across all sampled tasks after few-shot training:

$$\arg \min_{\theta} \sum_{\mathcal{T}_i \sim p(\mathcal{T}_i)} \mathcal{L}_{\mathcal{T}_i}(f_{\theta'_i}) = \sum_{\mathcal{T}_i \sim p(\mathcal{T}_i)} \mathcal{L}_{\mathcal{T}_i}(f_{\theta'_i = \theta - \alpha \nabla_{\theta} \mathcal{L}_{\mathcal{T}_i}(f_\theta)}) \quad (2.1)$$

Please note that equation 2.1 is a bi-level optimization problem. This is the standard setup for all gradient-descent based meta-learning algorithms. The training (support) and validation (query) datasets samples should not overlap.

MAML was found to be unstable, sensitive to deep architecture choices, and requires heavy tuning of hyper-parameters [16]. Additionally, extending MAML to many-shot regimes is impractical. Backpropagating through many inner loop steps suffers from vanishing gradients and stresses memory for the need to store intermediate steps gradients.

Various approaches were introduced to address the shortcomings of MAML. These include Forward-Mode Differentiation (FMD) which provides exact solutions and does not require the inner loop loss to be a function of the meta-knowledge optimized for [17, 18]. FMD is, however, not scalable with the meta-knowledge. Moreover, greedy online methods are another alternative [19, 20] but they suffer from short-horizon bias [21]. The most promising technique is using implicit gradients [14, 22]. They require the inner loop loss to be a function of the meta-knowledge. Therefore, they are mostly used in hyperparameters optimization which is our concern in this study. For a wider review, please refer to *Hospedales et. al, 2020* survey [10]. Implicit Meta-Learning is introduced in detail in chapter 3.

2.2 Semi-Supervised Learning

2.2.1 Overview

Semi-Supervised Learning (SSL) learns from both a labelled dataset $\mathcal{D} = \{(x, y)\}$ and unlabelled dataset of only input instance $\mathcal{U} = \{x\}$. SSL objective function is divided into two terms for each dataset:

$$\min_{\theta} \sum_{(x,y) \in \mathcal{D}} l_S(x, y, \theta) + \lambda \sum_{u \in \mathcal{U}} l_U(u, \theta) \quad (2.2)$$

where l_S is the standard supervised loss such as cross-entropy for classification, l_U is an unsupervised loss on the unlabelled dataset and λ is a hyperparameter. The unsupervised loss chosen gives rise to different SSL algorithms. Here, the focus is on SSL algorithms that benefited from Meta-Learning; especially Consistency Regularization (CR) and Proxy-Label (PL) Methods. For a full review, please to refer to [23]. More algorithms are also covered in this dissertation's proposal.

2.2.1.1 Proxy-Label Methods

First, PL methods use the unlabelled dataset by generating pseudo-labels \tilde{y} for each unlabelled instance by some heuristic. Most commonly a teacher network pre-trained on

a large labeled dataset such as ImageNet is used or a network trained on the available small annotated dataset. The pseudo-labels along with the small labelled dataset are in turn used together to train a student network using a supervised loss, i.e: $l_U(u, \theta) \equiv l_S(u, \tilde{y}, \theta)$. This approach was found to suffer from confirmation bias [24]. Recently, it was proposed to introduce uncertainty weight per each unlabelled sample in a transductive setting through a regularization term that motivates compactness and separation between classes [25].

2.2.1.2 Consistency Regularization

CR capitalizes on the unlabelled data using a different approach. It assumes that a base network's output should not change significantly if the unlabelled sample is perturbed or augmented. Unsupervised Data Augmentation, for example, uses AutoAugment and Back Translation [8]. The base network takes both the unlabelled sample and its augmented version as inputs. The unaugmented instance output is used as a pseudo-label. The unsupervised loss in equation 2.2 becomes the cross-entropy between the pseudo label and the soft labeled output of the augmented image. This loss regularizes the network to produce similar outputs to both original and augmented unlabelled instances. Hence, the network benefits from implicit information in the unlabelled dataset when learning. Additionally, CR techniques include FixMatch [6], MixMatch [26], ReMixMatch [9], Virtual Adversarial Training (VAR) [27] which all use the same assumption but slightly different augmentation strategies.

2.2.2 FixMatch

In this study, we use FixMatch as our base semi-supervised algorithm [6] whose backbone model is a deep network, f_θ , parameterized by θ . Therefore, the algorithm is explained briefly in this section as the necessary background for the rest of the report. Put simply, FixMatch uses two data augmentation strategies for the unlabelled instances. The two strategies are divided into a weak augmentation $\alpha(u)$ and a strong one $\mathcal{A}(u)$. The weak strategy is flipping an image horizontally with a probability of 50% and translating the image by up to 12.5% vertically or horizontally. Meanwhile, the strong augmentations used and evaluated were RandAugment [28] and CTAugment [9]. In this study, we only use RandAugment to simplify implementation and supplement initial comparisons with the baseline.

As shown in figure 2.1, each unlabelled image is augmented twice using both

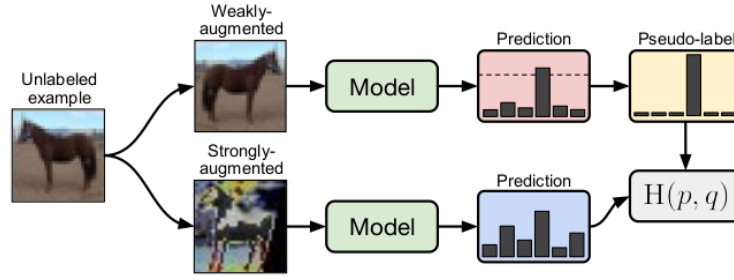


Figure 2.1: FixMatch Unsupervised Loss. [6]

weak and strong perturbations. Let $\alpha(u)$ denote the weak augmentation function on instance u , then the prediction, $q = f_{\theta}(y|\alpha(u))$, is used to produce a pseudo-label, $\hat{q} = \operatorname{argmax}(q)$, if the highest predicted class exceeds a threshold τ ; weak augmented images predictions are masked to only include confidently predicted instances. Subsequently, the unsupervised loss is the cross-entropy between the pseudo-label and the soft labelled output of the strong augmented image (regularizing the network to predict similar outputs to both strong and weak augmentations). The unsupervised loss per unlabelled image is then:

$$l_U(u) = \mathbb{1}(\max(q) \geq \tau) H(\hat{q}, f_{\theta}(y|\mathcal{A}(u))) \quad (2.3)$$

where $H(.,.)$ is the standard cross-entropy classification loss and $\mathcal{A}(u)$ is the strong augmentation on unlabelled image u . In summary, FixMatch combines both pseudo-labels and consistency regularization by design.

2.3 Meta-Learning for SSL

Meta Pseudo Labels (MPL) [11] was introduced to fix the confirmation bias of PL methods using the bi-level optimization formulation of Meta-Learning. MPL trains both the teacher and student network alternately to improve each other's performance. This alternating setup is mutually beneficial for both networks. First, the teacher generates pseudo labels which are used to train the student. Subsequently, the performance of the student is used as a signal to update the teacher parameters in the direction of the solution space which improves the student performance. However, producing pseudo-labels for all unlabelled images assumes that they are all equally beneficial with not out-of-domain samples.

Regarding Consistency Regularization, by referring to equation 2.2, one would note that all unlabelled instances are weighted equally by the hyperparameter λ . If unlabelled instances contain out-of-domain samples, weighting them equally would harm performance. Therefore, *Ren et al* proposed to learn a weight per each unlabelled image transductively [12].

2.4 Critique

To the best of the author’s knowledge, no study has previously attempted to learn to weigh unlabelled datapoints inductively for consistency regularization by extracting domain-centric visual features from the unlabelled images. Meta Pseudo Labels learns to label instances by assuming that they are equally beneficial. Furthermore, *Ren et al* learn instance wise weights transductively [12]. Similarly, in a self-supervised pre-training setting, *Ericsson et al.* learns to prune data transductively to minimize downstream tasks loss of a different domain [29]. The proposed method learns a probability distribution over the weight of each unlabelled instance.

Chapter 3

Implicit Meta-Learning

3.1 Overview

Implicit Meta-Learning (IML) has found great interest and success stories in recent literature on meta-learning for many-shot regimes. In particular, *Lorraine et al.* [14] have introduced Implicit Function Theorem to the meta-update rule. This allows the inner loop to train to convergence without having to unroll the trajectory of the inner-loop and backpropagate through all of this. First, the method is introduced.

In hyperparameters Optimization (HO), IML provides approximate gradients for the long inner loop trajectory of the baseline model training process. HO as a bi-level optimization problem is defined as:

$$\lambda^* = \arg \min_{\lambda} \mathcal{L}_V^*(\lambda), \text{ where} \quad (3.1)$$

$$\mathcal{L}_V^*(\lambda) := \mathcal{L}_V(\lambda, \mathbf{w}^*(\lambda)) \text{ and } \mathbf{w}^*(\lambda) := \arg \min_{\mathbf{w}} \mathcal{L}_T(\lambda, \mathbf{w}) \quad (3.2)$$

where \mathcal{L}_T and \mathcal{L}_V are training and validation losses respectively. The variables λ are the hyperparameters being optimized for and $\mathbf{w}^*(\lambda)$ are base model best-response parameters to the hyperparameters; that is training the base model till convergence given the hyperparameters. Using the chain rule to take the derivative of the validation loss with respect to (w.r.t) the hyperparameters, we get:

$$\frac{\partial \mathcal{L}_V^*}{\partial \lambda} = \left(\frac{\partial \mathcal{L}_V}{\partial \lambda} + \frac{\partial \mathcal{L}_V}{\partial \mathbf{w}} \frac{\partial \mathbf{w}^*}{\partial \lambda} \right) \Bigg|_{\lambda, \mathbf{w}^*(\lambda)} = \left(\frac{\partial \mathcal{L}_V(\lambda, \mathbf{w}^*(\lambda))}{\partial \lambda} + \frac{\partial \mathcal{L}_V(\lambda, \mathbf{w}^*(\lambda))}{\partial \mathbf{w}^*(\lambda)} \frac{\partial \mathbf{w}^*(\lambda)}{\partial \lambda} \right) \quad (3.3)$$

The three terms in equation 3.3 from left to right are: hyperparameters direct gradient, base model parameters direct gradient, and best-response Jacobian. In HO, the first

term is usually zero since the hyperparameters are not used during inference time (on the validation set). The second term is easily computable using automatic differentiation library as a standard routine in all machine learning algorithms. Finally, the Best-Response Jacobian provides information on how the weights have evolved and changed with respect to the hyperparameters used. It requires unrolled differentiation which as discussed earlier is problematic. Therefore, Implicit Function Theorem (IFT) is used in Lorraine’s approach.

Theorem 1 (Implicit Function Theorem). *Given regularity conditions, if $\frac{\partial \mathcal{L}_T}{\partial \mathbf{w}}|_{\lambda', \mathbf{w}'} = 0$ for some values (λ', \mathbf{w}') , then $\exists \mathbf{w}^*(\lambda)$ s.t. $\frac{\partial \mathcal{L}_T}{\partial \mathbf{w}}|_{\lambda, \mathbf{w}^*(\lambda)} = 0$ and*

$$\frac{\partial \mathbf{w}^*}{\partial \lambda} \Big|_{\lambda'} = - \left[\frac{\partial^2 \mathcal{L}_T}{\partial \mathbf{w} \partial \mathbf{w}^T} \right]^{-1} \times \frac{\partial^2 \mathcal{L}_T}{\partial \mathbf{w} \partial \lambda^T} \Big|_{\lambda', \mathbf{w}^*(\lambda')} \quad (3.4)$$

The condition of theorem 1 is equivalent to a fixed point in the base model training gradient field. If the base model is trained till convergence, then the condition hold, and IFT is used to avoid unrolled differentiation and find a local approximation to the best-response Jacobian. Implicit Meta-Learning is shown in algorithm 1.

Algorithm 1: Implicit Meta-Learning Algorithm

Input : Training Data \mathcal{D} , Validation Data \mathcal{V} .

Output: Optimal Hyperparameters λ^*

```

1 Initialize hyperparameters and base model parameters as  $\lambda$  and  $\mathbf{w}$  respectively
2 while Not Converged do
3   for  $t = 0 \dots T-1$  do
4      $\mathbf{w}^t = \alpha \cdot \frac{\partial \mathcal{L}_T}{\partial \mathbf{w}}|_{\lambda', \mathbf{w}'}$ 
5   end
6    $v_1 = \frac{\partial \mathcal{L}_V(\lambda, \mathbf{w}^*(\lambda^{(t)}))}{\mathbf{w}^*(\lambda^{(t)})}$ 
7   Approximate inverse Hessian-vector product,  $v_2 = v_1 \times \left[ \frac{\partial^2 \mathcal{L}_T}{\partial \mathbf{w} \partial \mathbf{w}^T} \right]^{-1}$ 
8    $v_3 = v_2 \times \frac{\partial^2 \mathcal{L}_T}{\partial \mathbf{w} \partial \lambda}$ 
9    $\lambda^{(t+1)}_- = \eta \times (-v_3) \rightarrow \lambda^{(t+1)}_+ = \eta \times v_3$ 
10 end

```

The algorithm involves computing the Inverse Hessian-vector product of the base model as per line 7. For deep neural networks, this computation is practically impossible memory-wise and is extremely computationally expensive. In the coming section, commonly used approximation methods for inverse Hessian-vector products are introduced and discussed while showing how they give rise to different algorithms.

3.2 Approximating Inverse Hessians

3.2.1 Neumann Series

Lorraine’s approach used Neumann Series to bypass the need to invert the Hessian matrix which requires cubic operations to the size of the matrix $O(n^3)$. The Neumann Series for an inverse Hessian is defined as:

$$\left[\frac{\partial^2 \mathcal{L}_T}{\partial \mathbf{w} \partial \mathbf{w}^T} \right]^{-1} = \lim_{i \rightarrow \infty} \sum_{j=0}^i \left[I - \frac{\partial^2 \mathcal{L}_T}{\partial \mathbf{w} \partial \mathbf{w}^T} \right]^j \quad (3.5)$$

The paper further shows that approximating this inverse using i terms in the Neumann Series is equivalent to unrolling differentiation for a trajectory of i steps around the local optimal weights of the base model. This theorem is re-stated in Theorem 2. They further show that storing the inverse Hessian in memory which is impractical can be detoured by utilizing an efficient vector-Hessian product. Theorem 2 gives rise to algorithm 2. The arxiv paper has a typo in line 4 ($p- = v$). The correct computation is $p+ = v$.

Theorem 2 (Neumann-SGD). *If we recurrently unroll Stochastic Gradient Descent (SGD) starting from $\mathbf{w}_0 = \mathbf{w}^*(\lambda)$, then*

$$\frac{\mathbf{w}_{i+1}}{\partial \lambda} = \left(\sum_{j < i} \left[I - \frac{\partial^2 \mathcal{L}_T}{\partial \mathbf{w} \partial \mathbf{w}^T} \right]^j \right) \frac{\partial^2 \mathcal{L}_T}{\partial \mathbf{w} \partial \lambda} \Bigg|_{\mathbf{w}^*(\lambda)} \quad (3.6)$$

and if $I + \frac{\partial^2 \mathcal{L}_T}{\partial \mathbf{w} \partial \mathbf{w}^T}$ is contractive, then as $i \rightarrow \infty$, the recurrence converges to eq. 3.4.

Algorithm 2: Neumann Series Approximation of the Inverse Hessian-vector Product

Input : Direct Validation Loss derivative w.r.t base model weights \mathbf{v} , direct Training Loss derivative w.r.t base model weights \mathbf{f} , base model weights \mathbf{w} and number of neumann steps i

Output: Inverse Hessian Vector Product, \mathbf{p}

- 1 Initialization: Store copy of validation loss direct gradient $\mathbf{p} = \mathbf{v}$
 - 2 **for** $j = 1 \dots i$ **do**
 - 3 $\mathbf{v}- = \alpha \times \text{grad}(\mathbf{f}, \mathbf{w}, \text{grad_outputs}=\mathbf{v})$
 - 4 $\mathbf{p}+=\mathbf{v}$
 - 5 **end**
-

3.2.2 Conjugate Gradient

Conjugate Gradient (CG) is a fabled algorithm for Hessian-free second order optimization [30,31]. The implemented version of CG in this study is based on lorraine's original Github implementation from their Data Augmentation experiments. In meta-learning terms, CG aims to approximate the inverse Hessian-vector product by solving the following equation:

$$\arg \min_{\mathbf{x}} \left\| \mathbf{x} \frac{\partial^2 \mathcal{L}_T}{\partial \mathbf{w} \partial \mathbf{w}^T} - \frac{\mathcal{L}_V}{\partial \mathbf{w}} \right\| \quad (3.7)$$

CG originally was derived from Newton's optimization method which solves an optimization problem through solving a sequence of local quadratic approximations of the function to update model parameters. Meanwhile, CG for conducting Hessian-Free Deep Learning optimization requires damping and pre-conditioning [32]. To minimize the degrees of freedom for CG algorithm and achieve comparable outcomes, Lorraine's implementation was depended on as said. The hyperparameters update rule is then:

$$\lambda^{(t+1)} = \lambda^{(t)} + \eta \left(\arg \min_{\mathbf{x}} \left\| \mathbf{x} \frac{\partial^2 \mathcal{L}_T}{\partial \mathbf{w} \partial \mathbf{w}^T} - \frac{\partial \mathcal{L}_V(\lambda^{(t)}, \mathbf{w}(\lambda))}{\partial \mathbf{w}(\lambda)} \right\| \right) \frac{\partial^2 \mathcal{L}_T}{\partial \mathbf{w} \partial \lambda^T} \Bigg|_{\lambda^{(t)}, \mathbf{w}^*(\lambda^{(t)})} \quad (3.8)$$

3.2.3 Identity Matrix For IML vs T1-T2

Finally, using the Identity matrix to approximate the Inverse Hessian gives rise to T1-T2 algorithm [15]. T1-T2 is a greedy algorithm. It updates the hyperparameters being optimized for after every single update for the base model parameters. Using the identity matrix simply means that the derivative of the weight with respect to the gradient is approximated as:

$$\frac{\partial \mathbf{w}}{\partial \lambda} \Bigg|_{\lambda'} = - \frac{\partial^2 \mathcal{L}_T}{\partial \mathbf{w} \partial \lambda^T} \Bigg|_{\lambda', \mathbf{w}(\lambda')} \quad (3.9)$$

Subsequently, the hypergradient using the following rule:

$$\lambda^{(t+1)} = \lambda^{(t)} + \eta \frac{\partial \mathcal{L}_V(\lambda^{(t)}, \mathbf{w}(\lambda))}{\partial \mathbf{w}(\lambda)} \frac{\partial^2 \mathcal{L}_T}{\partial \mathbf{w} \partial \lambda^T} \Bigg|_{\lambda^{(t)}, \mathbf{w}(\lambda^{(t)})} \quad (3.10)$$

The assumption of T1-T2 is that equation 3.10 approximates the hypergradient and the identity approximates the true Inverse Hessian. The method theoretically only converges when all components of the best-response Jacobian and mixed partial derivative are orthogonal. Therefore, there are no guarantees of convergence since machine learning optimization converges when gradients are theoretically zero. In theory, this

approximation is unjustified and will not strictly hold in practice. Nevertheless, in experiments where the base model is ResNet [33], for example, one might argue that the residual connections do bring the Hessian closer to the Identity.

An important distinction in terminology for the rest of the report is T1-T2 vs IFT-Identity (or simply referred to as Identity approximation). Whenever T1-T2 is used, then the algorithm alternates between the base model and meta-knowledge updates each step (one meta-update after every base model update). Otherwise, IFT-Identity is used when the base model is trained for many steps before taking a meta-update step whose hyper-gradient is computed by using the identity in place of the Inverse Hessian.

3.2.4 Note

Please note that discussed algorithms above are practically realizable as long as they depend on Hessian-Vector products. These are assumed to be easily computable without storing the actual Hessian in memory through Pearlmutter’s method [34].

3.3 Proposed Methodology

As stated earlier, it is unclear how different inverse-Hessian approximation methods influence and affect implicit meta-learning. Previous studies resort to comparisons of the approximations to the true inverse on over-simplified problems such as linear networks [14] or some fixed chosen random matrices. Otherwise, approximation methods accuracy with respect to the exact inverse Hessian of deep learning models, when studied in more depth, would only involve simplified tractable sub-problems such as only computing the exact inverse for the final layer of a deep ResNet [12]. It is unclear how these methods influence and affect the overall performance of solutions found when incorporated into the training procedure itself or how the approximations compare to the exact inverse as training proceeds and the loss landscape is being explored. Equally important, the overall cost of training using the approximations and their stability has been utterly overlooked and ignored in the literature.

We propose a comparative analysis between Neumann Series, Conjugate Gradient, IFT-Identity, and T1-T2 approximations to contrast empirically the pros and cons of each method. We admit a small model. A Multi-Layer Perceptron (MLP) with a single hidden layer and as many hidden neurons as inputs is chosen. Using MLP is selected to minimize the complexity of the problem, remove the influence of strong architecture

prior inductive biases, and enable computing exact inverse Hessians.

The meta-knowledges learnt are: 1) Per Parameter L_2 Regularizer and 2) Per Layer L_2 Regularizer. Meta-Knowledge (1) is an over-parameterization of the base model regularization. This is used to question whether using different approximations successfully overfits the validation (query) set. Overfitting the validation set translates to IML making the most out of available information in the validation data. Meta-knowledge (2) is a standard regularization technique that is used to improve base model generalization power by balancing the trade-off between learning from the validation set and improving base model generalization.

The hyperparameters were initialized randomly for both meta-knowledge. The weight decay values are kept positive by applying a Softplus non-linearity to them. The total regularization value is computed as: $[\text{Softplus}(\lambda) \odot \mathbf{w}]^2$ where \odot is a point-wise multiplication. The hyperparameters λ are either a matrix with the same shape as an MLP layer's parameters w (meta-knowledge 1) or a single element for each layer parameter's (meta-knowledge 2).

The metrics colligated on meta-knowledge (1) were 1) approximation accuracy with respect to exact inverse, 2) stability of the training procedure, 3) approximator influence on training procedure capacity (ability to overfit a small validation set), and 4) compute cost in terms of memory and time. For the memory metric, the maximum allocated memory for computing the inverse-Hessian vector product is measured. Meta-Knowledge (2) is used to test the generalization power of the solution found, algorithm stability, and again on compute cost. Each experiment setup was repeated three times on two datasets, namely MNIST [35] and CIFAR-10 [36] where the latter is a more challenging dataset than the former to learn using an MLP.

Chapter 4

Experiments and Results

For all experiments of this part of the project, the base model optimizer used was Adam [37] with a learning rate (LR) of 10^{-4} and RMSprop as the meta-knowledge optimizer with LR of 0.1 and default Pytorch values for all other parameters. Experiments were run on a single Tesla k80 GPU and each was repeated three times with different seeds.

4.1 Learning Per Parameter Regularizer

4.1.1 Training Details

For this problem setup, 50 samples were used per training, validation, and testing set. The inner loop was trained for 50 steps with batch sizes of 32 and meta-knowledge was updated 1000 times; 1000 epochs of 50 steps each, updating every epoch. For T1-T2, the model was trained for a total of 50K steps updating meta-knowledge after every step. The number of inner steps and batch size allow the base model performance to converge. Using few samples for training/validation enables investigating the power of approximation methods in using the validation set as stated earlier. This experiment follows directly from Lorraine’s investigation ([14], section 5.1). The number of Neumann Series terms studied were 3, 10, 20, 35, and 50. For CG, only 3, 5, and 10 steps were used because it has a heavy compute time cost as will be shown briefly.

4.1.2 Overfitting a Small Validation Set Results

The results are shown at table 4.1 and 4.2 for MNIST and CIFAR-10 datasets respectively. For Brevity, Neumann (3) and CG (3) will be used to respectively denote Neumann Series or CG approximations using 3 terms. It was found that if IML is trained

Table 4.1: **MNIST**: Mean and standard deviation of performance metrics for learning per parameter weight decay regularizer (overfitting small validation set) experiment. “ES Test” and “Test” are results of final model performances with and without early stopping. The increasing number of Neumann or CG steps produces instabilities. Neumann (3) is best performing method with IFT-Identity producing comparative results with less variance.

Name	Accuracy			
	Training	Validation	Test	ES Test
3 Step Neumann	100.00±0.00%	100.00±0.00%	64.00±2.83	77.33±4.11
10 Step Neumann	100.00±0.00%	88.00±5.66%	48.00±10.20	54.67±6.18
20 Step Neumann	100.00±0.00%	79.33±0.94%	56.00±10.71	60.00±6.53
35 Step Neumann	100.00±0.00%	91.33±5.73%	52.00±4.32	60.00±3.27
50 Step Neumann	98.00±2.83%	81.33±10.50%	37.33±19.48	56.00±5.89
3 Step CG	100.00±0.00%	94.67±0.94%	57.33±1.89	57.33±1.89
5 Step CG	99.33±0.94%	78.00±4.32%	62.00±3.27	52.67±0.94
10 Step CG	58.67±0.94%	40.00±2.83%	12.00±0.00	6.00±0.00
IFT-Identity	100.00±0.00%	94.00±1.63%	72.00±4.32	76.67±1.89
T1-T2	100.00±0.00%	96.00±1.63%	69.33±2.49	-

for long after convergence, then the validation and training accuracies start degrading. This behavior did not manifest in T1-T2. These dynamics are shown in appendix A along with more detailed experiment results. Therefore, the reported validation and training accuracies are the highest values achieved during the whole training procedure before degradation. Shortly, early stopping will be investigated as means for mitigating this issue. For comparison, results without and with early stopping are shown in columns “Test” and “ES Test”. “Test” accuracy is that of the final model after full training (at the end of 1000th epoch), while “ES Test” is evaluated on the model checkpoint of early stopping (model at the point where validation loss was at its lowest during the whole training before early stopping termination).

By looking at tables 4.1 and 4.2, one would notice that with the Neumann (3) approximation, the MNIST validation set is successfully overfitted. However, on the CIFAR-10 dataset, the same approximation would seem to not overfit. Nevertheless, CIFAR-10 results are over 3 repetitions of the experiment. Two out of the three experiments successfully overfitted the dataset except for a single experiment which on

Table 4.2: **CIFAR-10**: Mean and standard deviation of performance metrics for learning per layer weight decay regularizer experiment. “ES Test” and “Test” are results of final model performances with and without early stopping. CG (5) is the best performing method and again IFT-Identity produces competitive second to best performance.

Name	Accuracy			
	Training	Validation	Test	ES Test
3 Step Neumann	100.00±0.00%	86.00±19.80%	18.00±3.27	18.67±6.60
10 Step Neumann	100.00±0.00%	51.33±2.49%	15.33±0.94	20.00±2.83
20 Step Neumann	100.00±0.00%	35.33±17.46%	18.00±2.83	17.33±6.60
35 Step Neumann	95.33±0.94%	16.67±0.94%	14.67±0.94	14.00±1.63
50 Step Neumann	77.33±0.94%	18.00±0.00%	8.00±0.00	8.00±0.00
3 Step CG	100.00±0.00%	94.67±0.94%	20.00±3.27	23.33±1.89
5 Step CG	100.00±0.00%	92.00±0.00%	18.67±0.94	24.67±0.94
10 Step CG	82.67±5.25%	14.67±0.94%	4.00±0.00	10.00±0.00
IFT-Identity	100.00±0.00%	84.67±2.49%	20.00±2.83	21.33±0.94
T1-T2	100.00±0.00%	88.67±1.89%	20.67±1.89	-

the validation set reached a maximum validation of 58%. IFT-Identity and T1-T2 performances are surprisingly and consistently close to that of the best performing approximation - Neumann (3).

Increasing the number of Neumann terms paints the algorithm more unstable and exacerbates the ability of the model to overfit the validation set. When the average validation accuracy is high, as in Neumann (50) for MNIST, one would find that the variance is extremely high for an acceptable margin in Deep Learning training. Similarly, increasing the number of CG steps worsens its’ performance. This counter-intuitive observation will be studied and explained in section 4.1.3 with relation to the method’s ability in approximating the loss function curvature after convergence.

Generalization Power: As previously stated, if the training procedure is trained further after overfitting the validation set, a catastrophic forgetting occurs; both validation loss and accuracy start worsening. Therefore, all the above experiments were repeated with early stopping conditioned on the validation loss not improving for 15 meta-updates. All method’s generalization power improves if we condition the training on the validation loss except for CG (5)&(10) on MNIST and Neumann (20)&(35) on CIFAR-10. This further worsening of performance is because those particular methods

either exhibit very high variance regarding how long the method takes before converging or are unstable. The first issue means that the method could stuck in a local optimum for a while before escaping again and early stopping is placed to terminate too soon. However, this is a sign of the approximation method being unrobust. Robustness of training convergence speed and stability of approximating inverse Hessian-vector products are discussed and investigated further in sections 4.1.4 and 4.1.3 respectively. One can safely conclude that it would be a beneficial practice to *place early stopping on validation loss when learning some meta-knowledge using Implicit Meta-Learning*.

The best performing methods are Neumann (3) and CG (5) on MNIST and CIFAR-10 respectively. Solutions produced by the IFT-Identity approximation are second best. Nevertheless, they overall have equal or lower variance than the best solution found. Hence IFT-Identity has consistently produced stable and consistent performance across both datasets, despite not over-fitting the validation data. T1-T2 generalization is unclear (better than Neumann(3) on CIFAR-10 and worse on MNIST). This will be investigated further in section 4.2 experiments.

4.1.3 Approximation Methods Comparison to Exact Inverse Hessian-Vector Product

Computing the Hessian and its exact inverse was impossible for a simple MLP network on the MNIST dataset. It requires allocating **1.55 Terabytes** for an MLP with 784 input and hidden neurons. Therefore, a smaller MLP with 32 hidden neurons was used to enable computing the exact Hessian and its inverse. Furthermore, using the full resolution of MNIST made computing the inverse unstable, therefore the images were resized down to 14×14 pixels. Using the convention of reporting the highest validation loss achieved, summary performance statistics are shown in table 4.3. The validation losses are healthier and greater than expected for the small capacity of the MLP employed here. Therefore, conclusions made here can be extrapolated to the full setting with larger MLPs. Finally, using the same setup of learning per MLP weight L_2 regularizer on MNIST, the exact inverse Hessian-vector product was computed every 5 meta-updates giving 20 comparisons in total. Computing the exact inverse of the Hessian was sometimes unstable throwing CUDA overflow exceptions among others. Hence, unstable computations were discarded. Comparisons are shown in figure 4.2

Observation 1: *Increasing Neumann Series terms worsens its accuracy:*

Table 4.3: **MNIST** - Per Weight Regularizer with Small MLP Experiment (reporting mean and std values). “Best Step @” is a synonym to Convergence Epoch from previous tables. Computing the inverse of the exact Hessian was occasionally unstable. Hence, the absence of its results.

Name	Accuracy			
	Training	Validation	Test	Best Step @
3 Step Neumann	43.33±1.89%	42.00±6.53%	19.33±2.49	15.00±5.10
10 Step Neumann	44.00±3.27%	46.67±4.99%	25.33±8.38	19.33±7.41
20 Step Neumann	51.33±6.18%	43.33±4.99%	27.33±12.26	40.33±26.71
35 Step Neumann	41.33±3.40%	38.00±4.90%	18.00±2.83	18.00±5.35
50 Step Neumann	45.33±6.18%	38.00±6.53%	31.33±12.26	40.33±40.37
3 Step CG	54.00±6.53%	52.67±6.60%	34.00±7.12	69.00±36.25
5 Step CG	58.67±0.94%	47.33±2.49%	40.00±0.00	54.33±33.51
Identity	52.00±2.83%	42.67±6.60%	31.33±5.25	38.00±40.32

To understand why, please note that Neumann Series is an iterative shrinking of the direct validation loss gradient (algorithm 2). By assumption, the base model was trained until convergence and hence its validation loss gradient is already extremely small. Therefore, Neumann Series introduces sparse matrix multiplication in the hypergradient calculation, and increasing Neumann terms quickly introduce vanishing gradients. Moreover, the shrinking is administered by subtracting a weighted and exponentiated Hessian-vector product where the vector multiplied by is the direct validation loss. The weight, α is set to a default of 0.1. Therefore, these multiple exponentiations and weighting of matrices with low norms quickly introduce floating-point errors among other numerical stabilities. These factors altogether produced the phenomenon evident in figure 4.1.

Observation 2: *Catastrophic forgetting observed when IML is trained beyond convergence can be explained in terms of the accuracy of estimating inverse Hessian-vector products:*

Neumann(3) only exhibits high variance after the algorithm convergences. Few Neumann terms provide the most consistent and robust estimate. This variance in estimating the inverse Hessian-Vector product is one source of explanation to why training and validation performance worsens and the need for early stopping.

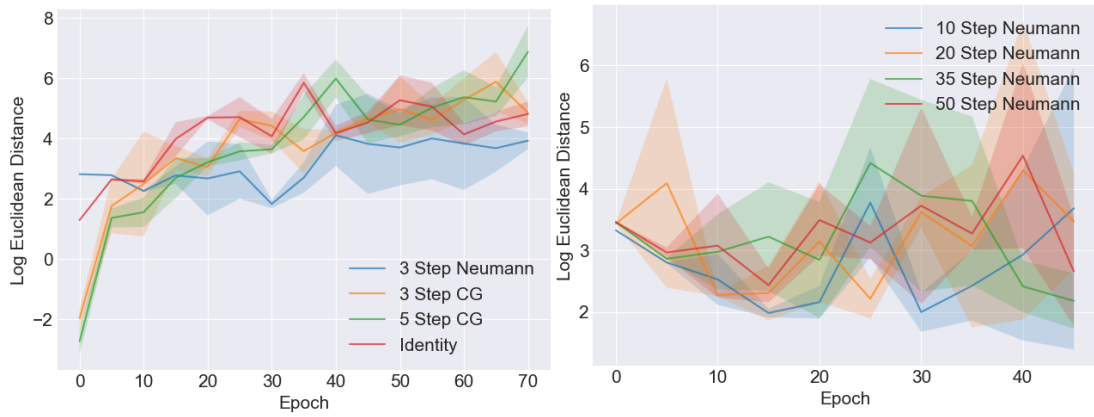


Figure 4.1: Comparison of approximations methods with respect to exact inverse Hessian-vector product.

4.1.4 Compute Cost

Memory Consumption: All methods consume a constant pre-allocated memory for approximation functions calls. Memory costs are shown in table 4.4. Since multiplying by Identity yields the same matrix, then the inverse Hessian-vector product computation is skipped and no extra memory is allocated for it. Hence, the memory cost for the Identity approximation is zero. Regarding table 4.4, note that memory costs difference between Neumann and CG unclear on the MNIST dataset materialize on CIFAR-10. This is because the CIFAR-10 images have 3 channels each with more pixels than the one channeled MNIST images.

Compute time needed for the experiments on both both MNIST and CIFAR-10 are shown in table 4.5 and 4.6 respectively. For T1-T2, measurements are computed over 50 steps to normalize comparison metrics. The epoch column is the time taken for the whole meta-

Table 4.4: Maximum memory allocated for the function calls computing the inverse Hessian-vector product for both MNIST and CIFAR-10 datasets in Mega, Giga, and Terabytes (Mb, Gb, Tb). Both Neumann Series and CG allocate constant memory irrespective of the number of iterations/terms. Row “Exact” denotes the exact Hessian computation.

Name	Data	Memory
Neumann	MNIST	58.35 Mb
Neumann	CIFAR-10	875 Mb
CG	MNIST	73.18 Mb
CG	CIFAR-10	1101 Mb
Identity	MNIST	0.0
Identity	CIFAR-10	0.0
Exact	MNIST	1554 Gb
Exact	CIFAR-10	358 Tb

Table 4.5: **MNIST**: Per Weight Regularizer Experiment Time Cost. Reported values are mean and standard deviations measured in milliseconds for “time cost”.

Name	Time Cost		
	Epoch	Approximation	Convergence Epoch
3 Step Neumann	186.34±4.68 ms	5.18±0.04 ms	133.33±47.84
10 Step Neumann	191.01±1.43 ms	16.45±0.07 ms	30.67±2.62
20 Step Neumann	200.90±1.30 ms	31.96±0.20 ms	24.67±1.25
35 Step Neumann	226.15±0.29 ms	56.31±0.10 ms	35.33±8.34
50 Step Neumann	248.78±1.59 ms	80.03±0.56 ms	31.33±11.26
3 Step CG	164.26±1.17 ms	16.60±0.06 ms	155.33±133.41
5 Step CG	169.49±0.46 ms	25.94±0.07 ms	354.33±168.69
10 Step CG	193.15±0.46 ms	49.86±0.10 ms	0.00±0.00
Identity	175.03±1.14 ms	0.20±0.01 ms	146.33±77.81
T1-T2	464.00±6.5 ms	0.22±0.00 ms	409.00±215.99
Exact Hessian	-	120.15±211.83 s	-

epoch to run, including the inner loop steps, full hypergradient computation, and meta-update. The Approximation column is the time taken for approximating the inverse Hessian-vector product. Finally, the Convergence Epoch is the total number of epochs taken to achieve the best validation error as reported previously.

The approximation time taken as a ratio of the whole epoch time grows as we use more Neumann terms and CG steps. For high-performing methods such as Neumann (3), the approximation time is negligible; 3% of the whole epoch time. Expectedly, T1-T2 epoch time is the most expensive method as hypergradients are computed every single step of the epoch. The highest cost of Implicit Meta-Learning is the time taken to train the base model to convergence in all stable and high-performing methods. This conclusion will be revisited in meta-knowledge (2) experiments where the full datasets are used in a standard machine learning routine that aims to improve generalization. When using a similar number of iterations, CG is approximately three times slower than Neumann. Focusing on a well-performing method such as Neumann(3) for both MNIST and CIFAR-10, one would note that they converge slower than most methods but while yielding better overall performance. As expected, there exists a trade-off between the training time taken of each approximation method and the respective quality

Table 4.6: **CIFAR-10**: Per Weight Regularizer Experiment Time Cost. Reported values are mean and standard deviations measured in milliseconds for “time cost”.

Name	Time Cost		
	Epoch	Approximation	Convergence Epoch
3 Step Neumann	797.01±0.21 ms	22.98±0.01 ms	106.33±47.59
10 Step Neumann	850.93±0.06 ms	76.67±0.01 ms	17.33±2.49
20 Step Neumann	927.41±0.83 ms	153.37±0.05 ms	113.33±106.15
35 Step Neumann	1043.40±0.15 ms	268.60±0.05 ms	2.67±2.05
50 Step Neumann	1164.73±0.54 ms	382.50±0.19 ms	2.00±0.00
3 Step CG	870.17±0.10 ms	97.23±0.11 ms	118.00±24.10
5 Step CG	929.13±0.20 ms	156.83±0.24 ms	159.33±15.84
10 Step CG	1089.78±0.75 ms	307.33±0.12 ms	1.33±0.47
Identity	774.08±0.05 ms	0.00±0.00 ms	132.00±67.15
T1-T2	2124.50±2.00 ms	0.00±0.00 ms	165.79.33±52.62

of the solution found. The more stable a method is, the more time it takes before converging to produce better solutions. Close-performing methods take an approximately similar number of epochs to converge with IFT-Identity taking the most number of epochs to converge.

What seems to be fast Convergence in some methods is in effect a sign of instability. For example, CG (10), which consistently produced random test performances, appears to converge early. This translates to the validation loss being highest after initialization before being degraded by training. Finally, there is a discrepancy in the inner loop cost when using the IFT-Identity approximation for the MNIST dataset. It is slower than CG (3) and CG (5) for example. As all experiments are run sequentially on a K80 GPU, this outlier is potentially due to CUDA not freeing some cores or resources properly at some point before that experiment and hence it ends up using fewer resources.

4.2 Learning Per Layer Regularizer

4.2.1 Training Details

This problem setup is studied to dig deeper into the generalization power of different solutions found by the approximation methods. The full training MNIST and CIFAR-10 datasets were used with their standard train/test split. The testing set was split by half for both the validation and test set which produces 5000 samples each. Batch size used was 128 samples per base model update. For the meta-update, the training and validation losses were computed on the full available data although it was found that using a small random sample of 500 instances for each gives a great approximation for the true losses.

Initially, IML was found to be unstable on the CIFAR-10 dataset producing random predictions. This only happened when inner loop steps are “not long enough”. In an attempt to reduce the number of inner loop steps needed, the base model was initialized using converged parameters of pre-training using the respective dataset. With this initialization, the threshold of “enough steps” found for the base model training reduced but varied between methods. Inspecting the base model weights after meta-updates showed that when using inner training steps less than the found “enough” steps which vary among methods then all model parameters vanish quickly making the network weight matrices extremely sparse.

This problem was pinpointed to be an early underestimation of the training loss in the first meta-epoch. That is, once the model starts training using the hyperparameters, the training loss initially decreases before jumping drastically again. The thresholds established manually were exactly the steps needed to reach that jump. In summary, if the base model is updated too early, the loss of the hyperparameters initialization is underestimated, assumed well-performing and the meta-update takes a step in the wrong meta-loss direction destabilizing the base model performance.

Warm-Up Training Procedure: We propose to train the base model to convergence with the initialized hyperparameters before doing meta-updates. This enables the training loss to stabilize and converge. It was found that this warm-up training procedure stabilizes the base model training as long as the warm-up training allows the jump to occur. Furthermore, it was found that every meta-update does not take the base model new loss far away from convergence, and hence the number of inner loop steps needed for the base model to converge are half that of the warm-up convergence.

The experiments discussed in this section had a 1000 step warm-up training of the base

Table 4.7: **MNIST** - Per layer regularizer experiment statistics (reporting mean and standard deviations). The baseline reported here used no regularization as it was found that Grid Searching for an L_2 did not produce better solutions (grid search results are in appendix A.2).

Name	Accuracy		
	Training	Validation	Test
Baseline	94.78±0.10%	94.82±0.24%	94.42±0.13
3 Step Neumann	99.41±0.03%	98.05±0.05%	98.14±0.10
10 Step Neumann	99.32±0.01%	97.97±0.07%	98.02±0.00
20 Step Neumann	99.22±0.02%	97.89±0.03%	97.95±0.01
35 Step Neumann	99.07±0.02%	97.80±0.02%	97.91±0.03
50 Step Neumann	98.84±0.01%	97.65±0.05%	97.80±0.06
3 Step CG	99.44±0.02%	98.25±0.07%	98.06±0.04
5 Step CG	99.26±0.10%	98.15±0.01%	98.17±0.07
10 Step CG	33.73±25.44%	34.34±25.47%	10.73±0.22
Identity	99.45±0.02%	98.06±0.07%	98.10±0.08
T1-T2	23.38±2.86%	23.25±2.81%	10.15±0.92

model with initialized hyperparameters which brings the model to convergence. Additionally, the number of inner loop steps used was 500 which allows the base model to converge after every single meta-update. Meta-knowledge was updated 50 times except for T1-T2 where the base model and meta-updates alternates (50×500 total updates each). Generalization power and compute cost are again discussed. Finally, an ablation study in section 4.2.4 investigates how varying the number of inner loop steps for training the base model influences the solution found.

4.2.2 Generalization Power

Results are shown in tables 4.8 and 4.7. Meta-Learning improves over baseline models generalization for both datasets when using either Neumann (3) or CG (3). Results for optimizing a single regularization value for the baseline using grid search are added in appendix A.2. None of the searched for values performed any better than the baseline performance reported without regularization in tables 4.7 and 4.8 which shows how hard it is to optimize such simple hyperparameters.

Observations Summary: Neumann (3) and CG (3) improve over baselines in both

Table 4.8: **CIFAR-10** - Per Layer Regularizer Experiment Statistics. The baseline reported here used no regularization as it was found that Grid Searching for an L_2 did not produce better solutions (grid search results are in appendix A.2).

Name	Accuracy		
	Training	Validation	Test
Baseline	58.25±0.19%	51.72±0.13%	50.39±0.50
3 Step Neumann	98.64±0.25%	55.63±0.03%	55.12±0.04
10 Step Neumann	34.69±4.54%	35.11±4.35%	34.13±4.74
20 Step Neumann	30.80±2.58%	31.49±2.08%	28.39±3.61
35 Step Neumann	28.57±0.97%	29.77±0.74%	23.41±0.56
50 Step Neumann	27.88±2.12%	28.84±1.78%	23.88±0.88
3 Step CG	98.77±0.24%	56.40±0.29%	54.83±0.53
5 Step CG	35.59±3.90%	36.31±4.02%	28.29±12.87
10 Step CG	18.50±2.15%	18.57±2.59%	10.16±0.00
Identity	98.59±0.39%	55.69±0.18%	55.02±0.82
T1-T2	99.91±0.01%	56.41±0.22%	55.37±0.56%

MNIST and CIFAR-10 experiments. Consistent with findings of the previous section, increasing Neumann series or CG iterations degrades performance, using CG introduces higher variance than Neumann series does, and using the IFT-Identity approximation yields competitive results to best-performing methods on both experiments.

Stability Issues: Some seeds for the MNIST experiments produced unstable results across all approximations and it was hard to find working seeds. Therefore, some of these results are over two repetitions of the experiments. The exception is T1-T2 on MNIST which as shown in table 4.7 is unstable producing random predictions across all seeds. The observed algorithm instability only occurred on the MNIST dataset.

Conclusion: When the meta-knowledge learned is not over-parameterized, training beyond validation loss convergence does not worsen performance. The Validation and Test performance are comparatively close which shows that choosing reasonable hyperparameters as the meta-knowledge does not overfit but rather improves performance over baseline. The improvement over baselines is significantly larger than what one would expect on both datasets.

4.2.3 Compute Cost

Memory Cost: In 4.9, memory consumed is much higher than the overfitting a small validation set experiments although the meta-knowledge learned is smaller. This is a direct result of the batch sizes being four times larger and approximations retaining the backpropagation graphs in memory during each step. In addition, unlike the previous experiments, Neumann series is using a higher memory than CG in this setup although not significantly larger. This is a direct result of copying the accumulated validation loss gradient (algorithm 2) which is produced for a set 500 times larger than before.

Time cost for CIFAR-10 in learning per layer

L_2 regularization weight is shown in table 4.10. Focusing on a well-performing method such as Neumann(3), the approximation only takes 25% of the total meta-iteration time. Therefore, as the inner loop task becomes more complex, the most costly training overhead is allowing the base model to converge. Even though the proposed warm-up procedure helps reduce the number of inner loop steps taken to converge by half, it is still costly to run both the warm-up and inner loop to convergence routines in modern models such as ViT [38]. Therefore, when repeatedly training the base model till convergence is impractical, one would resort to using fewer base model training steps. In the next section, an ablation study that simulates such a situation is conducted.

Table 4.9: Maximum memory allocated for the function calls computing the inverse Hessian-vector product for both MNIST and CIFAR-10 datasets. Both Neumann Series and CG allocate constant memory irrespective of the number of iterations/terms

Name	Data	Memory
Neumann	MNIST	1.6 GB
Neumann	CIFAR-10	5.6 Gb
CG	MNIST	1.4 Gb
CG	CIFAR-10	5.2 Gb
Identity	MNIST	0.0
Identity	CIFAR-10	0.0

4.2.4 Ablation Study

Varying Inner Steps: Same warm-up procedure was run as explained earlier to eliminate the instability associated with initialization and control comparison. The training steps of the base model after each meta-update were varied from 50 to 500 steps (starting with 50, 100 and then up to 500 with 100 step increments). To simulate the situation where compute resources are scarce, the number of meta-updates are kept constant

Table 4.10: **CIFAR-10** - Per Layer Regularizer Experiment Time Cost.

Name	Time Cost		
	Epoch	Approximation	Convergence Epoch
3 Step Neumann	12.99±5.03 s	3.10±0.20 s	30.33±5.56
10 Step Neumann	20.25±28.86 s	10.36±3.59 s	32.00±19.20
20 Step Neumann	30.64±17.30 s	20.75±8.72 s	5.33±2.87
35 Step Neumann	46.20±30.45 s	36.29±49.78 s	16.67±18.62
50 Step Neumann	61.80±128.05 s	51.88±108.90 s	4.00±0.82
3 Step CG	18.79±19.24 s	9.65±6.26 s	36.33±6.55
5 Step CG	23.99±812.48 s	14.91±742.76 s	32.33±21.48
10 Step CG	35.78±32.13 s	26.84±29.19 s	0.33±0.47
Identity	9.86±67.73 s	0.00±0.00 s	41.67±5.25
T1-T2	55±75 s	0.00±0.00 s	30.426±10.41

(50 total updates) while decreasing base model training steps. Comparing accuracies across models trained for different number of total steps is conducted to directly assess how much accuracy is sacrificed in such situations where computational resources are scarce. In the case of T1-T2, the question becomes if reducing total number of training steps while meta-updating after each inner loop step is necessary in comparison to updating less frequently as in IFT-Identity. Results are shown in figure 4.2.

First, starting from 100 inner loop steps with 50 meta-updates, the validation loss, and hence the outer loop, converges for all methods (plots included in appendix B). Therefore, learning stability of the meta-knowledge is not sensitive to the number of inner loop steps. Using fewer steps only affects the quality of the solution found. Note that all methods shown in the right plot of figure 4.2 are not consistently improving over the baseline. Meanwhile, methods in the left plot are always outperforming the baseline. Concerning the left plot, T1-T2 is occasionally performing better than IFT-Identity and Neumann (3) but not consistently. To make the most of using T1-T2, one has to figure out the optimal steps needed to train the base model for which is costly and challenging. As shown in table 4.10, the compute cost of each 500 T1-T2 steps is at least 4x that of Neumann (3) and at least 5x of IFT-Identity.

With the noise present in the base model losses estimation, T1-T2 explores the meta-loss landscape much more aggressively with unnecessary overhead. On the other hand, training the base model for longer provides a better estimation of the meta-

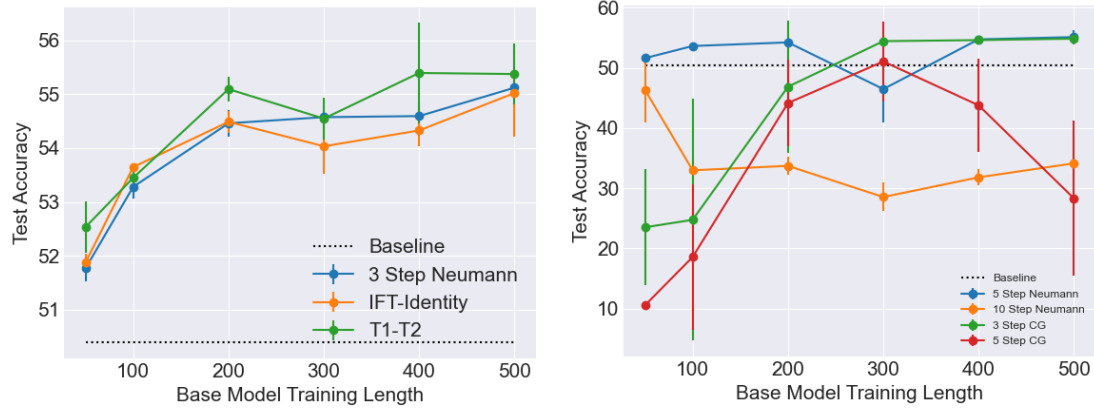


Figure 4.2: Generalization power of IML for Learning Per Layer L_2 Regularizer weight on the CIFAR-10 Dataset when using different inverse Hessian-vector product approximation methods while varying number of base model training steps.

knowledge performance which produces a better hypergradient direction allowing each meta-update to navigate the meta-loss more efficiently reaching a solution faster at the expense of slightly lower performance.

4.3 Discussion

4.3.1 Summary

A great deal of attention has been given recently to Implicit Gradients for Meta-Learning (IML) [12, 14, 22]. Such methods require computing second-order derivatives which are impractical for modern-day Deep Learning models. Previous research resort to various approximation methods to estimate such inverse Hessian-Vector products. In this chapter, these approximation methods, namely CG, Neumann Series, and IFT-Identity, were compared and contrasted in terms of compute cost, stability, generalization power, and utilization power of the available validation data. T1-T2 [15] as a famous method was too investigated. First, the problem of overfitting a small validation set was used to study how different approximations utilize the validation set. Overfitting was induced by learning a separate L_2 regularization weight for each network parameter. Then, learning an L_2 regularization weight per each network layer experiment was conducted using the full datasets to investigate how or if IML improves

over baseline generalization.

We have shown that when trying to overfit a small validation set, IML succeeds to do so with Neumann (3). Nevertheless, catastrophic forgetting phenomenon is always produced by IFT updates if trained beyond convergence. This was shown to be directly linked to the inability of IFT to approximate the curvature of the loss landscape accurately. The Hessian approximations beyond convergence had high variances leading the meta-update to move away from the space of the solution found. This observation is particularly of interest to the continual learning research [39]. In addition, we have shown how using more terms or iterations for Neumann Series or CG produces worse solutions and destabilizes training.

Generalization-wise, IFT-Identity was consistently producing performances at par with the best performing method in any experiment. Gain in performance for T1-T2 in comparison with less frequent updating methods such as IFT-Identity seems insignificant when the cost of the updates is reckoned with. Finally, the memory cost of all methods grows with respect to the base model batch sizes, and hence size of accumulated gradients, rather than with the size of the meta-knowledge itself. Moreover, in such experiments, training the base model to convergence becomes the highest computational cost of the experiment. Warm-up training allows reducing the inner loop number of steps needed to converge. Using fewer inner loop steps and breaking the convergence assumption still produces results that improve over the baselines without affecting meta-knowledge training stability and convergence.

4.3.2 Critique and Future Work

The approximation methods' influence on shaping the loss landscape has not been studied in this dissertation. Recently, the influence of various network architecture elements and training procedures on deep learning dynamics was studied through the lens of the evolution of the Hessian during training [40–42]. With the release of recent libraries providing fast computations of the eigenvalue decomposition of deep network Hessians [43], one can better examine the sources of catastrophic forgetting observed in IML, investigate the degrading estimation ability of different approximation methods as training proceeds and question how the approximations shape and get shaped back by the loss landscape. Insights gained from such an exploration can be used to design better approximation methods, potentially produce a new method altogether or help design a new regularization scheme for the meta-loss itself.

Chapter 5

Confidence Network for FixMatch

5.1 Introduction

Recent best performing Semi-Supervised Learning (SSL) algorithms [7,11] place equal importance on all available unlabelled datapoints. It was found, however, that the performance of SSL algorithms substantially worsen when the unlabelled dataset contains out-of-distribution or out-of-domain samples [44]. Therefore, recent attempts to address this problem has focused on learning a per instance transductive weight that reflects the importance of such sample for improving the SSL algorithm’s performance [12].

We propose here a novel SSL algorithm that learns to inductively weigh unlabelled instances by learning a direct representation which maps images to importance/relevance weights. In a meta-learning setting, we initiate and train a Confidence Network, $C(u; \omega)$, parameterized by ω , whose output resembles how confident is the CN that the unlabelled image, u , would improve base classifier performance. We conjecture that such setup would allow the CN to extract domain-centric features from unlabelled images, u , prune out-of-distribution data and further use the representation to transfer knowledge to other downstream tasks. Preliminary results show that our original proposed method improves FixMatch baseline performance and learns to discerns unlabelled images relevance to the domain being studied.

The problem formulation, learning rules and algorithm are introduced in section 5.2. Experiment setup, training details and results are covered in section 5.3. Subsequently, the learnt representation is interrogated and investigated in section 5.4 to answer the question: “What did the Confidence Network really learn?”. Finally, critique of the current proposal and directions for further work are covered in section 5.5.

5.2 Algorithm

For semi-supervised setting with meta-learning, available data is divided into three sets; a fully labelled training data $\mathcal{D} = \{(x, y)\}$, an unlabelled set $\mathcal{U} = \{u\}$ and a validation set $\mathcal{V} = \{(x, y)\}$. The base classifier is a deep network $f_\theta(x)$, parameterized by θ and the Confidence Network learns to weigh unlabelled datapoints to improve base classifier performance. More formally, the following bi-level optimization problem is addressed (base model parameters dependence on CN parameters is denoted $\theta^*(\omega)$):

$$\omega^* = \arg \min_{\omega} \mathcal{L}_s(\mathcal{V}, \theta^*(\omega)) = \frac{1}{|\mathcal{V}|} \sum_{i=1}^{|\mathcal{V}|} \mathcal{L}_s^{(i)}(\theta^*(\omega)) \quad (5.1)$$

$$\begin{aligned} \theta^*(\omega) &= \arg \min_{\theta} \mathcal{L}^{train}(\mathcal{D}, \mathcal{U}, \theta, \omega) \\ &= \arg \min_{\theta} \mathcal{L}_s(\mathcal{D}; \theta) + \sum_{u \in \mathcal{U}} C(\alpha(u); \omega) \mathcal{L}_u(u; \theta) \end{aligned} \quad (5.2)$$

Please recall that FixMatch unsupervised loss was defined as $\mathcal{L}_u(u; \theta) = \mathbb{1}(\max(q) \geq \tau) H(\hat{q}, f_\theta(y | \mathcal{A}(u)))$ where $\alpha(u)$ and $\mathcal{A}(u)$ are FixMatch weak and strong augmentation respectively on images u , $q = f_\theta(y | \alpha(u))$, $\hat{q} = \arg \max(q)$, and $\mathbb{1}(\max(q) \geq \tau)$ filters out poor pseudo-labels. Weak augmentations include translation and rotation while strong ones are RandAugment [28].

Update Rules: the base model and confidence network parameters update rules at step t are:

$$\omega^{(t+1)} = \omega^{(t)} - \beta \nabla_{\omega} \mathcal{L}_s(\mathcal{V}; \theta(\omega^*)) \quad (5.3)$$

$$\theta^{(t+1)} = \theta^{(t)} - \frac{\alpha}{n} \left[\nabla_{\theta^{(t)}} \mathcal{L}_s(\mathcal{D}; \theta^{(t)}) + \sum_{u \in \mathcal{U}} C(\alpha(u); \omega) \nabla_{\theta^{(t)}} \mathcal{L}_u(u; \theta) \right] \quad (5.4)$$

Meta-Knowledge Update Rule: Using Implicit Meta-Learning from *Lorraine et al.* [14], the Confidence Network parameters updates rules can be derived as:

$$\frac{\partial \mathcal{L}_s^*(\mathcal{V}, \theta^*(\omega))}{\partial \omega} = \frac{\mathcal{L}_s(\mathcal{V}, \theta^*(\omega))}{\partial \omega} + \frac{\partial \mathcal{L}_s(\mathcal{V}, \theta^*(\omega))}{\partial \theta^*(\omega)} \frac{\partial \theta^*(\omega)}{\partial \omega} \quad (5.5)$$

where

$$\frac{\partial \theta^*(\omega)}{\partial \omega} = - \left[\frac{\partial^2 \mathcal{L}^{train}}{\partial \theta \partial \theta^T} \right]^{-1} \times \frac{\partial \mathcal{L}^{train}}{\partial \theta \partial \omega^T} \Big|_{\omega', \theta^*(\omega')} \quad (5.6)$$

Therefore, equation 5.3 becomes:

$$\begin{aligned} \omega^{(t+1)} &= \omega^{(t)} + \beta \left[\frac{\partial \mathcal{L}_s(\mathcal{V}, \theta^*(\omega))}{\partial \theta^*(\omega)} \times \left[\frac{\partial^2 \mathcal{L}^{train}}{\partial \theta \partial \theta^T} \right]^{-1} \times \frac{\partial \mathcal{L}^{train}}{\partial \theta \partial \omega^T} \Big|_{\omega', \theta^*(\omega')} \right] \\ &= \Theta^{(t+1)} + \beta \left[\frac{\partial \mathcal{L}_s(\mathcal{V}, \theta^*(\omega))}{\partial \theta^*(\omega)} \times \left[\frac{\partial^2 \mathcal{L}^{train}}{\partial \theta \partial \theta^T} \right]^{-1} \times \frac{\partial C(\alpha(u), \omega) \mathcal{L}_u}{\partial \theta \partial \omega^T} \Big|_{\omega', \theta^*(\omega')} \right] \end{aligned} \quad (5.7)$$

Meta-Update Rule Interpretation: Equation 5.7 shows how the update rule orients the meta-parameters towards the ascent direction of the validation loss gradient. This is further weighted by the unsupervised loss gradient which reflects how increasing an unlabelled datapoint confidence in the batch affects that validation loss. The full training routine is shown in algorithm 3.

Algorithm 3: Fixing FixMatch by Confidence Network Weighting Algorithm

Input : Training Data \mathcal{D} , Validation Data \mathcal{V} , Unlabelled Data \mathcal{U} , batch sizes $n, p, m=|\mathcal{V}|$ and max iterations T .

Output: Classifier Network Parameters: $\theta^*(\omega^*)$ and Weighting Network parameters: ω^*

- 1 Initialize Classifier and Confidence Networks parameters as $\omega^{(0)}$ and $\Theta^{(0)}$ respectively
- 2 **while** *Not Converged* **do**
- 3 **for** $t = 0 \dots T-1$ **do**
- 4 $\{x, y\} \leftarrow \text{SampleMiniBatch}(\mathcal{D}, n)$
- 5 $\{x^{\mathcal{U}}\} \leftarrow \text{SampleMiniBatch}(\mathcal{U}, p)$
- 6 Update classifier network parameters using eq 5.3
- 7 **end**
- 8 $v_1 = \frac{\partial \mathcal{L}_s(\mathcal{V}, \omega^*(\Theta^{(t)}))}{\omega^*(\Theta^{(t)})}$ using the validation dataset
- 9 Approximate inverse Hessian-vector product, $v_2 = v_1 \times \left[\frac{\partial^2 \mathcal{L}^{train}}{\partial \theta \partial \theta^T} \right]^{-1}$
- 10 $v_3 = v_2 \times \frac{\partial \mathcal{C}(u; \omega) \mathcal{L}_u(u; \theta)}{\partial \theta \partial \omega} \Big|_{\omega', \theta^*(\omega')}$
- 11 $\frac{\partial \mathcal{L}_s^*(\mathcal{V}, \omega^*(\Theta))}{\partial \Theta} = -v_3$
- 12 Compute $\Theta^{(t+1)}$ using update rule, equation 5.4
- 13 **end**

5.3 Evaluation and Results

5.3.1 Training Details

Experiment Setup: the proposed method is evaluated on the CIFAR-10 dataset. We use 250 labelled training images (25 instances per class), a validation set of size 1000 (100 instances per class) and the full training data without the validation set as unlabelled data. A relatively large validation set is being used as per the convention of *Ren et al.* paper [12] which places an extra annotation overhead in standard SSL. In the

Critique and Further work section, a solution is proposed to remedy this concern.

Evaluation Study Control: the base model trained with CN would have implicit knowledge of extra labelled datapoints granting an unfair comparison to the baseline. Therefore, the CN was first trained, parameters producing best validation loss were saved and the trained base model was discarded. Then, the same 250 labelled training instances were used to train two FixMatch models from scratch with and without the saved CN. This strategy enables discerning the CN influence on FixMatch by comparing two models trained using the same data.

Training Details: With reference to line 1 in algorithm 3, the Classifier and Confidence Networks parameters are initialized randomly. Then, a warm up routine is run to bring the Confidence Network initialization to equally weigh all unlabelled datapoints. Using a target of 1 for all unlabelled images, the Confidence Network is trained for a fixed number of steps to extract heterogeneous features from the full available data that would result in all Confidence Network predictions to be close to 1.

Confidence and Classifier (base model) network architecture employed was ResNet-28 [45]. Both networks were trained using SGD with momentum and weight decay of 5×10^{-5} . The Classification and Confidence Networks learning rates were 0.03 and 1×10^{-3} respectively. For CN, higher learning rates were also tried but were found to produce a slightly worse accuracy on the validation set.

FixMatch exhibits the same dynamics observed in the learning per layer L_2 regularization weight where the unsupervised loss increases initially before decreasing again. Therefore, the base model was trained for 210 epochs in total where the first 10 epochs were a warm-up phase allowing the unsupervised loss to stabilize. This is followed by a meta-update. Subsequently, the base model is trained for 200 epochs, updating the Confidence Network after each 5 epochs. Updating the Confidence Network after each epoch produced worse performance than updating less frequently. FixMatch also exhibits very high noise per epoch, therefore each epoch is 512 steps. In summary, after warm-up and its respective meta-update, the base model is trained for a total of 102400 steps, updating the meta-knowledge after each 2560 steps.

Approximating the inverse-Hessian vector product was also challenging. The Neumann Series was found to be extremely unstable when trained with and without warm-up epochs. The Confidence Network starts producing weights up to a magnitude of 200 and oscillating aggressively down to negative values and up again. Therefore, IFT-Identity approximation was resorted to. T1-T2 was attempted with and without warm-up steps, updating after each inner loop step but was too found to be unstable;

the CN predicted values oscillated aggressively between 120 and -10 in consecutive steps.

Finally, as per equation 5.2, the Confidence Network consumes weakly augmented images during training and original images for either the validation set or during inference when parameters are fixed. Using the weakly augmented images during training introduces variability of exposure during learning as the image augmentations are applied with probabilities. This exposes the CN to knowledge on how the augmentation is directly influencing the overall training loss.

5.3.2 Results

Note: CN takes approximately 16-18 hours to train for 210 epochs on a Tesla A100 Tensor-Core GPU. Given short timescale of the project, it was only feasible to provide three repetitions of the experiments as reported here for our method and the baseline.

The results in table 5.1 show how our method improves over the baseline FixMatch performance. Please note that on experiment cifar10@250_3 which uses random number generator seed=3, proposed method did not perform better than the baseline. It was found that the validation loss of the CN of that experiment, although monotonically decreasing, was still significantly lower than other seeds. Therefore, training for longer could have potentially improved over the baseline or a different seed would have been chosen.

Next questions would be what did the Confidence Network actually learn? What weights is it producing and how does those weights vary among instances? These questions are the topic of the next section. The issue that the Confidence Network requires extra labelled datapoints to train is addressed in section 5.5.

Table 5.1: Preliminary experimental results using only 250 labelled datapoints from the CIFAR-10 dataset. Results are reported with a Confidence Weighting Network (ours) and without (FixMatch baseline). The results shown are over three repetitions.

Name	Baseline Test Accuracy	Ours
cifar10@250_1	93.69	94.04
cifar10@250_2	93.54	93.71
cifar10@250_3	93.23	91.13

5.4 What did the model learn?

To better understand the learnt representation of the Confidence Network, CN weights were produced for all original and weakly augmented images. All Confidence Networks produced during training were evaluated to also inspect how the outputs evolve as training proceeds. Please note that the CNs used in this section are those produced by experiment `cifar10@250_1` in table 5.1.

The comparison is shown in figure 5.1. A sign for training health is the evolution of the confidence weights produced; monotonic increase before convergence. The confidence weights produced by CN for the original images is on average higher in magnitude than the Weakly Augmented. The closeness of averages can be explained in terms of the low probabilities used in the weak augmentations of FixMatch as stated earlier. Some images evaluated in the weakly augmented settings would have not been actually augmented with some probability.

One would expect that the weakly augmented images outputs be significantly lower. This is revealed in the high variance exhibited in the weakly augmented instances outputs. The variance of the weights reaches a magnitude as low as 2.50 which the original images output is far from. Therefore, the Confidence Network does learn to distinguish and discriminate between “clear” and noisy instances.

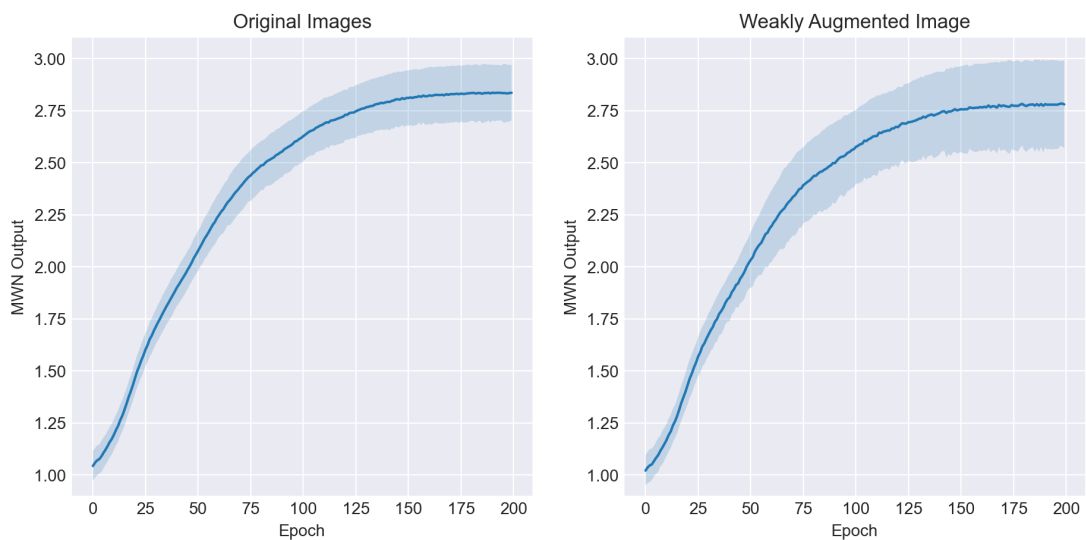


Figure 5.1: Average and standard deviation of weights produced by Confidence Networks for original and weakly augmented images as training proceeds.

Next, we select and visualize three images per each class by the highest, median and lowest weights predicted by trained Confidence Network as per figure 5.2. The highest and lowest weighed images are interpreted as images which the Confidence Network is most certain would increase and decrease base model performance respectively. The image with median prediction of CN is also included.

Note that the images with the highest inlier predictions, around the weight of 4, are all instances where the background colour is either solid or non-distracting, i.e: Truck, Frog, Airplane, Dog, Truck, Ship and Bird are all examples of this. The Confidence Network has chosen to upweigh an Automobile instance where the background is non-distracting, the car

front is clear and the car colors are contrasting and downweighs instances where the angle is found to be confusing to the base network for classification. Finally, the median and weakest weights predicted are close to each other. Therefore, next we visualize the distribution of weights predicted over the whole training data.

The histogram over all CN predictions is in figure 5.3. Note that the CN again upweighs very few instances consistently with the observation in figure 5.2. The average weights predicted lump around same values as in figure 5.1.

In conclusion, compelling evidence for the conjecture that the Confidence Network learns to weigh unlabelled images using domain-centric feature extraction has been provided. Some shortcomings in our proposed methodology are pinpointed in the next section. Further work to improve the algorithm is also introduced.

Plane				Car			
	4.21	2.82	2.44		4.04	2.83	2.48
	Bird					Cat	
3.79		2.78	2.34	4.38	2.78		2.40
Deer					Dog		
	3.84	2.77	2.41	4.43		2.79	2.45
	Frog					Horse	
4.24		2.76	2.42	3.89	2.81		2.45
Ship					Truck		
	3.92	2.81	2.47	4.03		2.83	2.44

Figure 5.2: From left to right per each class, the images with most, median and lowest weights predicted by Confidence Net are visualized. The number above below image is the CN predicted weight for the image

5.5 Conclusion and Further Work

Proposed method was shown to outperform FixMatch baselines. The interpretation of the Confidence Network in section 5.4 inspire using this formulation for other use cases such as out-of-distribution detection or domain adaptation and generalization.

Main shortcoming of the proposed method is the need of an extra labelled validation set. This can be addressed in two steps. First, eliminating the need for the labelled training data can be done using contrastive pre-training as proposed in SelfMatch [7]. The training labelled

data responsibility is to bring the base model to predict labels for the unlabelled instances with high confidence which SelfMatch solves using contrastive learning pre-training. Secondly, an ablation of the validation data size effect on base model performance must be conducted. If the Confidence Network is found to be data hungry, one potential solution would be sharing parameters between both Confidence network and base model. Then, only the final few convolutional and fully connected layers in the Confidence Network can be trained which would demand less data for the fewer trainable parameters. The final few layers of convolutional neural network are known to specialize more in domain knowledge than the initial ones. Therefore, the same interpretation instigated in this chapter can be carried forward to the new setup.

Finally, CIFAR-10 does not contain out-of-distribution or out-of-domain data because it was is curated with precision. Therefore, the full power of the proposed method was not conveyed or challenged. We propose to evaluate this method on a more challenging benchmark such as STL-10 which contains out-of-distribution images by design [46].

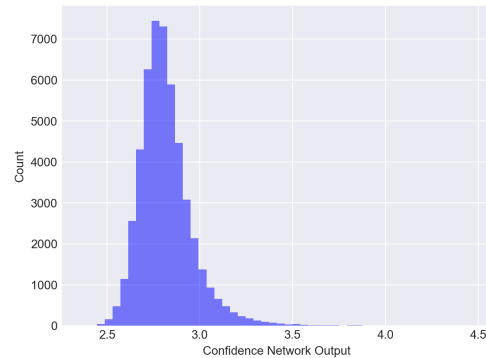


Figure 5.3: Histogram over all weight predictions by the Confidence Network for the full training dataset

Chapter 6

Conclusion

6.1 Summary and Reflection

Implicit meta-learning (IML) is great in solving vanishing gradient problems and high memory costs associated with standard meta-learning. In this research, we systematically compared the largely ignored evaluation of the effect of incorporating different second order gradient approximation methods into implicit meta-learning. Approximation methods studied were Neumann series, CG and T1-T2 approximations. The methods were contrasted in terms of compute cost, generalization power, stability and power to capitalize on the available validation data.

We have also shown that implicit meta-learning exhibits catastrophic forgetting phenomenon if trained for few epochs after convergence. This was explained in terms of the different approximation methods inability to estimate the curvature of the loss function (2^{nd} order gradient) at convergence which steers the meta-knowledge away from the solution found. Additionally, instability of IML associated with under-estimation of losses after meta-knowledge initialization was discovered and presented. A simple warm-up training procedure for initializing the base model parameters was proposed and evaluated to show that it successfully remedies the problem.

In the following part of the thesis, insights gained were used to design a novel semi-supervised learning algorithm which learns to weigh the consistency regularization losses of FixMatch inductively by a *Confidence Network* (CN). Intuitively, CN consumes images and outputs weights reflecting how confident is the network that the instance would improve FixMatch performance. We have shown that our proposed algorithm improves over FixMatch baseline performance. Additionally, we provide compelling evidence that the CN does indeed extract domain-centric features by vi-

sualizing the distribution of its outputs over the training data and providing example images up and down weighted. Few images with approximately twice the weight than the median output of the network were found to be ones without any distracting background information where feature extraction is much easier.

6.2 Future Work

For the comparative analysis, we proposed to study how the different inverse Hessian-vector product approximations shape and get shaped back by the meta-loss function. An initial methodology can follow the lines of recent studies which have investigated how different architecture element and training procedures such as batch sizes affect the loss surface [40–42]. There is availability of powerful tools to help such direction. For example, PyHessian provides PyTorch wrapper functions to easily and quickly compute eigenvalue decomposition, trace or highest eigenvalues of the loss function Hessian [43].

For our proposed semi-supervised learning algorithm, we proposed to start with an ablation study of the effect of the validation set size on algorithm performance. Thereafter, SelfMatch [7] can be used in place of FixMatch to eliminate the need of a training labelled data through contrastive pre-training. To reduce the validation set size further, sharing base model and CN parameters for the first few layers can be attempted. Finally, a dataset such as STL-10 which contains out-of-distribution samples by design should be used to produce a better evaluation of the proposed method and challenge its power.

Bibliography

- [1] Ian Goodfellow. *Deep learning*. The MIT Press, Cambridge, Massachusetts, 2016.
- [2] Y. Lecun, L. Bottou, Y. Bengio, and P. Haffner. Gradient-based learning applied to document recognition. *Proceedings of the IEEE*, 86(11), 1998.
- [3] Alex Krizhevsky, Ilya Sutskever, and Geoffrey E Hinton. Imagenet classification with deep convolutional neural networks. In *Advances in Neural Information Processing Systems*, volume 25, 2012.
- [4] Ashish Vaswani, Noam Shazeer, Niki Parmar, Jakob Uszkoreit, Llion Jones, Aidan N. Gomez, Lukasz Kaiser, and Illia Polosukhin. Attention is all you need, 2017.
- [5] Geoffrey Hinton, Li Deng, Dong Yu, George E. Dahl, Abdel-rahman Mohamed, Navdeep Jaitly, Andrew Senior, Vincent Vanhoucke, Patrick Nguyen, Tara N. Sainath, and Brian Kingsbury. Deep neural networks for acoustic modeling in speech recognition: The shared views of four research groups. *IEEE Signal Processing Magazine*, 29(6), 2012.
- [6] Kihyuk Sohn, David Berthelot, Chun-Liang Li, Zizhao Zhang, Nicholas Carlini, Ekin D. Cubuk, Alex Kurakin, Han Zhang, and Colin Raffel. Fixmatch: Simplifying semi-supervised learning with consistency and confidence. *CoRR*, 2020.
- [7] Byoungjip Kim, Jinho Choo, Yeong-Dae Kwon, Seongho Joe, Seungjai Min, and Youngjune Gwon. Selfmatch: Combining contrastive self-supervision and consistency for semi-supervised learning, 2021.
- [8] Qizhe Xie, Zihang Dai, Eduard Hovy, Minh-Thang Luong, and Quoc V. Le. Un-supervised data augmentation for consistency training, 2020.

- [9] David Berthelot, Nicholas Carlini, Ekin D. Cubuk, Alex Kurakin, Kihyuk Sohn, Han Zhang, and Colin Raffel. Remixmatch: Semi-supervised learning with distribution alignment and augmentation anchoring, 2020.
- [10] Timothy Hospedales, Antreas Antoniou, Paul Micaelli, and Amos Storkey. Meta-learning in neural networks: A survey, 2020.
- [11] Hieu Pham, Qizhe Xie, Zihang Dai, and Quoc V. Le. Meta pseudo labels. *CoRR*, abs/2003.10580, 2020.
- [12] Zhongzheng Ren, Raymond A. Yeh, and Alexander G. Schwing. Not all unlabeled data are equal: Learning to weight data in semi-supervised learning, 2020.
- [13] Chelsea Finn, Pieter Abbeel, and Sergey Levine. Model-agnostic meta-learning for fast adaptation of deep networks, 2017.
- [14] Jonathan Lorraine, Paul Vicol, and David Duvenaud. Optimizing millions of hyperparameters by implicit differentiation, 2019.
- [15] Jelena Luketina, Mathias Berglund, Klaus Greff, and Tapani Raiko. Scalable gradient-based tuning of continuous regularization hyperparameters. In *Proceedings of The 33rd International Conference on Machine Learning*, volume 48, 2016.
- [16] Antreas Antoniou, Harrison Edwards, and Amos Storkey. How to train your maml, 2019.
- [17] Luca Franceschi, Michele Donini, Paolo Frasconi, and Massimiliano Pontil. Forward and reverse gradient-based hyperparameter optimization. In *Proceedings of Machine Learning Research*, volume 70, 2017.
- [18] Paul Micaelli and Amos Storkey. Non-greedy gradient-based hyperparameter optimization over long horizons, 2021.
- [19] Hanxiao Liu, Karen Simonyan, and Yiming Yang. DARTS: Differentiable architecture search. In *International Conference on Learning Representations*, 2019.
- [20] Atilim Gunes Baydin, Robert Cornish, David Martinez Rubio, Mark Schmidt, and Frank Wood. Online learning rate adaptation with hypergradient descent. In *International Conference on Learning Representations*, 2018.

- [21] Yuhuai Wu, Mengye Ren, Renjie Liao, and Roger Grosse. Understanding short-horizon bias in stochastic meta-optimization. In *International Conference on Learning Representations*, 2018.
- [22] Aravind Rajeswaran, Chelsea Finn, Sham Kakade, and Sergey Levine. Meta-learning with implicit gradients, 2019.
- [23] Yassine Ouali, Céline Hudelot, and Myriam Tami. An overview of deep semi-supervised learning, 2020.
- [24] Eric Arazo, Diego Ortego, Paul Albert, Noel E. O’Connor, and Kevin McGuinness. Pseudo-labeling and confirmation bias in deep semi-supervised learning. In *2020 International Joint Conference on Neural Networks (IJCNN)*, July 2020.
- [25] Weiwei Shi, Yihong Gong, Chris Ding, Zhiheng MaXiaoYu Tao, and Nanning Zheng. Transductive semi-supervised deep learning using min-max features. In *Proceedings of the European Conference on Computer Vision (ECCV)*, September 2018.
- [26] David Berthelot, Nicholas Carlini, Ian Goodfellow, Nicolas Papernot, Avital Oliver, and Colin A Raffel. Mixmatch: A holistic approach to semi-supervised learning. In H. Wallach, H. Larochelle, A. Beygelzimer, F. d’Alché-Buc, E. Fox, and R. Garnett, editors, *Advances in Neural Information Processing Systems*, volume 32. Curran Associates, Inc., 2019.
- [27] Takeru Miyato, Shin ichi Maeda, Masanori Koyama, and Shin Ishii. Virtual adversarial training: A regularization method for supervised and semi-supervised learning, 2018.
- [28] Ekin Dogus Cubuk, Barret Zoph, Jon Shlens, and Quoc Le. Randaugment: Practical automated data augmentation with a reduced search space. In *Advances in Neural Information Processing Systems*, volume 33, 2020.
- [29] Linus Ericsson, Henry Gouk, and Timothy M. Hospedales. Don’t wait, just weight: Improving unsupervised representations by learning goal-driven instance weights, 2020.
- [30] R.K. Mehra. Computation of the inverse hessian matrix using conjugate gradient methods. *Proceedings of the IEEE*, 57(2), 1969.

- [31] James Martens and Ilya Sutskever. *Training Deep and Recurrent Networks with Hessian-Free Optimization*. Springer Berlin Heidelberg, Berlin, Heidelberg, 2012.
- [32] James Martens. Deep learning via hessian-free optimization. In *Proceedings of the 27th International Conference on International Conference on Machine Learning, ICML'10*, Madison, WI, USA, 2010. Omnipress.
- [33] Kaiming He, Xiangyu Zhang, Shaoqing Ren, and Jian Sun. Deep residual learning for image recognition. In *2016 IEEE Conference on Computer Vision and Pattern Recognition (CVPR)*, 2016.
- [34] Barak Pearlmutter. Fast exact multiplication by the hessian. *Neural Computation*, 6, 02 1970.
- [35] Li Deng. The mnist database of handwritten digit images for machine learning research. *IEEE Signal Processing Magazine*, 29(6), 2012.
- [36] Alex Krizhevsky. Learning multiple layers of features from tiny images. *University of Toronto*, 05 2012.
- [37] Diederik P. Kingma and Jimmy Ba. Adam: A method for stochastic optimization, 2017.
- [38] Alexey Dosovitskiy, Lucas Beyer, Alexander Kolesnikov, Dirk Weissenborn, Xiaohua Zhai, Thomas Unterthiner, Mostafa Dehghani, Matthias Minderer, Georg Heigold, Sylvain Gelly, Jakob Uszkoreit, and Neil Houlsby. An image is worth 16x16 words: Transformers for image recognition at scale. In *International Conference on Learning Representations*, 2021.
- [39] Antreas Antoniou, Massimiliano Patacchiola, Mateusz Ochal, and Amos Storkey. Defining benchmarks for continual few-shot learning, 2021.
- [40] Behrooz Ghorbani, Shankar Krishnan, and Ying Xiao. An investigation into neural net optimization via hessian eigenvalue density. In *Proceedings of the 36th International Conference on Machine Learning*, volume 97, 2019.
- [41] Zhewei Yao, Amir Gholami, Kurt Keutzer, and Michael W. Mahoney. Hessian-based analysis of large batch training and robustness to adversaries. NIPS, 2018.

- [42] Guillaume Alain, Nicolas Le Roux, and Pierre-Antoine Manzagol. Negative eigenvalues of the hessian in deep neural networks, 2018.
- [43] Zhewei Yao, Amir Gholami, Kurt Keutzer, and Michael Mahoney. Pyhessian: Neural networks through the lens of the hessian, 2020.
- [44] Avital Oliver, Augustus Odena, Colin Raffel, Ekin D. Cubuk, and Ian J. Goodfellow. Realistic evaluation of deep semi-supervised learning algorithms, 2019.
- [45] Sergey Zagoruyko and Nikos Komodakis. Wide residual networks, 2017.
- [46] Adam Coates, Andrew Ng, and Honglak Lee. An analysis of single-layer networks in unsupervised feature learning. In *Proceedings of the Fourteenth International Conference on Artificial Intelligence and Statistics*, volume 15, 2011.

Appendix A

Overfitting a Small Validation Set

A.1 Detailed Experiment Results

Naming conventions for tables in this section are as follows:

1. numn_3_sd_231 or CG_3_sd_231 means that 3 terms/steps were used for Neumann or CG respectively and sd_231 means that the experiment was set with seed=231 to initialize the random number generator of pytorch
2. Per Weight (Full 1000 epochs) tables: reporting final results of the base model after the full 1000 epochs for overfitting a small validation set experiments.
3. Per Weight (Early Stopping) tables: overfitting a small validation set with early stopping experiments results
4. Per Weight Resized tables: results of the approximation methods comparison with respect to exact inverse Hessian-vector product experiments
5. Per Layer tables are detailed results for the generalization experiments
6. To differentiate this Appendix's tables from those in the body of the document, the final validation performance rather than maximum achieved is reported here

Table A.1: MNIST - Per Weight (Full 1000 epochs).

Exp	Accuracy			Training Cost			
	Training	Validation	Test	Convergence Epoch	Approximation Time	Meta-Epoch Time T	Max Memory
numn_no_3_sd_231	100.00%	98.00%	66.00%	110	5.24 ms	192.95 ms	58.35 mb
numn_no_3_sd_981	100.00%	90.00%	60.00%	200	5.15 ms	183.29 ms	58.35 mb
numn_no_3_sd_1110	100.00%	98.00%	66.00%	90	5.15 ms	182.77 ms	58.35 mb
numn_no_10_sd_231	100.00%	56.00%	62.00%	27	16.54 ms	192.87 ms	58.35 mb
numn_no_10_sd_981	100.00%	50.00%	44.00%	33	16.44 ms	190.77 ms	58.35 mb
numn_no_10_sd_1110	100.00%	60.00%	38.00%	32	16.37 ms	189.39 ms	58.35 mb
numn_no_20_sd_231	100.00%	66.00%	58.00%	23	31.85 ms	200.13 ms	58.35 mb
numn_no_20_sd_981	100.00%	54.00%	42.00%	25	32.24 ms	202.73 ms	58.35 mb
numn_no_20_sd_1110	100.00%	66.00%	68.00%	26	31.79 ms	199.84 ms	58.35 mb
numn_no_35_sd_231	100.00%	60.00%	48.00%	28	56.34 ms	226.08 ms	58.35 mb
numn_no_35_sd_981	100.00%	62.00%	58.00%	47	56.41 ms	226.54 ms	58.35 mb
numn_no_35_sd_1110	100.00%	54.00%	50.00%	31	56.18 ms	225.83 ms	58.35 mb
numn_no_50_sd_231	100.00%	58.00%	48.00%	26	79.25 ms	246.55 ms	58.35 mb
numn_no_50_sd_981	12.00%	10.00%	10.00%	21	80.32 ms	249.63 ms	58.35 mb
numn_no_50_sd_1110	100.00%	56.00%	54.00%	47	80.53 ms	250.16 ms	58.35 mb
CG_3_sd_231	100.00%	78.00%	56.00%	60	16.64 ms	165.24 ms	73.18 mb
CG_3_sd_981	100.00%	76.00%	60.00%	62	16.65 ms	164.91 ms	73.18 mb
CG_3_sd_1110	100.00%	76.00%	56.00%	344	16.52 ms	162.62 ms	73.18 mb
CG_5_sd_231	100.00%	70.00%	62.00%	210	26.04 ms	170.11 ms	73.15 mb
CG_5_sd_981	96.00%	68.00%	58.00%	591	25.86 ms	169.03 ms	73.18 mb
CG_5_sd_1110	100.00%	72.00%	66.00%	262	25.92 ms	169.32 ms	73.18 mb
CG_10_sd_231	14.00%	16.00%	12.00%	0	50.00 ms	193.80 ms	73.15 mb
CG_10_sd_981	14.00%	16.00%	12.00%	0	49.77 ms	192.91 ms	73.18 mb
CG_10_sd_1110	14.00%	16.00%	12.00%	0	49.81 ms	192.75 ms	73.18 mb
identity_sd_231	100.00%	82.00%	66.00%	255	0.20 ms	176.09 ms	38.53 mb
identity_sd_981	100.00%	78.00%	74.00%	77	0.19 ms	175.53 ms	38.53 mb
identity_sd_1110	100.00%	84.00%	76.00%	107	0.21 ms	173.45 ms	38.53 mb
tl12_sd_231	100.00%	90.00%	70.00%	33802	0.22 ms	9.45 ms	2.71 mb
tl12_sd_981	100.00%	86.00%	66.00%	20196	0.22 ms	9.24 ms	2.71 mb
tl12_sd_1110	100.00%	78.00%	72.00%	7352	0.22 ms	9.14 ms	2.71 mb

Table A.2: MNIST - Per Weight (Early Stopping).

Exp	Accuracy			Training Cost			
	Training	Validation	Test	Convergence Epoch	Approximation Time	Meta-Epoch Time T	Max Memory
numn_no_3_sd_231	100.00%	100.00%	82.00%	110	5.39 ms	197.44 ms	58.35 mb
numn_no_3_sd_981	100.00%	100.00%	72.00%	200	5.32 ms	195.25 ms	58.35 mb
numn_no_3_sd_1110	100.00%	100.00%	78.00%	90	5.33 ms	195.54 ms	58.35 mb
numn_no_10_sd_231	88.00%	68.00%	60.00%	27	18.68 ms	206.96 ms	58.35 mb
numn_no_10_sd_981	92.00%	70.00%	46.00%	33	17.78 ms	204.53 ms	58.35 mb
numn_no_10_sd_1110	96.00%	68.00%	58.00%	32	18.19 ms	203.99 ms	58.35 mb
numn_no_20_sd_231	88.00%	68.00%	52.00%	23	35.03 ms	217.03 ms	58.35 mb
numn_no_20_sd_981	100.00%	74.00%	68.00%	25	33.82 ms	214.43 ms	58.35 mb
numn_no_20_sd_1110	92.00%	72.00%	60.00%	26	32.78 ms	212.69 ms	58.35 mb
numn_no_35_sd_231	100.00%	74.00%	60.00%	28	56.80 ms	235.50 ms	58.35 mb
numn_no_35_sd_981	96.00%	74.00%	64.00%	47	55.97 ms	234.47 ms	58.35 mb
numn_no_35_sd_1110	100.00%	66.00%	56.00%	31	55.53 ms	233.03 ms	58.35 mb
numn_no_50_sd_231	100.00%	68.00%	64.00%	26	78.74 ms	253.42 ms	58.35 mb
numn_no_50_sd_981	94.00%	66.00%	50.00%	21	78.87 ms	253.53 ms	58.35 mb
numn_no_50_sd_1110	92.00%	76.00%	54.00%	47	79.14 ms	255.11 ms	58.35 mb
CG_3_sd_231	100.00%	90.00%	56.00%	64	16.75 ms	167.23 ms	73.18 mb
CG_3_sd_981	100.00%	94.00%	60.00%	50	16.73 ms	166.92 ms	73.18 mb
CG_3_sd_1110	100.00%	92.00%	56.00%	70	16.82 ms	167.04 ms	73.18 mb
CG_5_sd_231	98.00%	54.00%	52.00%	51	26.29 ms	172.95 ms	73.18 mb
CG_5_sd_981	98.00%	54.00%	54.00%	69	26.26 ms	172.98 ms	73.18 mb
CG_5_sd_1110	98.00%	50.00%	52.00%	20	26.00 ms	171.52 ms	73.18 mb
CG_10_sd_231	16.00%	6.00%	6.00%	0	49.98 ms	197.46 ms	73.15 mb
CG_10_sd_981	16.00%	6.00%	6.00%	0	50.01 ms	197.67 ms	73.18 mb
CG_10_sd_1110	16.00%	6.00%	6.00%	0	50.01 ms	197.26 ms	73.18 mb
identity_sd_231	100.00%	94.00%	74.00%	85	0.23 ms	181.57 ms	38.53 mb
identity_sd_981	100.00%	92.00%	78.00%	77	0.23 ms	180.88 ms	38.53 mb
identity_sd_1110	100.00%	94.00%	78.00%	107	0.23 ms	181.30 ms	38.53 mb
tl12_sd_231	10.00%	12.00%	2.00%	12	0.21 ms	25.82 ms	2.71 mb
tl12_sd_981	8.00%	10.00%	12.00%	11	0.23 ms	9.51 ms	2.71 mb
tl12_sd_1110	16.00%	24.00%	20.00%	11	0.20 ms	9.57 ms	2.71 mb

Table A.3: MNIST - Per Weight Resized.

Exp	Accuracy			Training Cost			
	Training	Validation	Test	Convergence Epoch	Approximation Time	Meta-Epoch Time T	Max Memory
numn_3_sd.231	32.00%	20.00%	22.00%	13	4.56 ms	159.10 ms	0.75 mb
numn_3_sd.981	24.00%	38.00%	20.00%	10	4.47 ms	153.75 ms	0.75 mb
numn_3_sd.1110	28.00%	28.00%	16.00%	22	4.48 ms	153.28 ms	0.75 mb
numn_10_sd.231	18.00%	16.00%	14.00%	26	14.16 ms	161.72 ms	0.75 mb
numn_10_sd.981	42.00%	26.00%	34.00%	9	14.25 ms	163.31 ms	0.75 mb
numn_10_sd.1110	28.00%	32.00%	28.00%	23	14.17 ms	163.30 ms	0.75 mb
numn_20_sd.231	46.00%	22.00%	28.00%	19	27.80 ms	174.78 ms	0.75 mb
numn_20_sd.981	60.00%	38.00%	42.00%	78	27.52 ms	173.53 ms	0.75 mb
numn_20_sd.1110	32.00%	24.00%	12.00%	24	27.67 ms	174.20 ms	0.75 mb
numn_35_sd.231	18.00%	24.00%	14.00%	19	48.87 ms	197.49 ms	0.75 mb
numn_35_sd.981	26.00%	30.00%	20.00%	11	48.08 ms	194.49 ms	0.75 mb
numn_35_sd.1110	28.00%	40.00%	20.00%	24	48.56 ms	196.52 ms	0.75 mb
numn_50_sd.231	20.00%	26.00%	16.00%	18	69.75 ms	218.50 ms	0.75 mb
numn_50_sd.981	42.00%	22.00%	32.00%	6	69.52 ms	218.21 ms	0.75 mb
numn_50_sd.1110	54.00%	46.00%	46.00%	97	69.35 ms	217.32 ms	0.75 mb
CG_3_sd.231	46.00%	38.00%	30.00%	18	15.86 ms	164.27 ms	0.91 mb
CG_3_sd.981	60.00%	60.00%	44.00%	90	15.83 ms	163.93 ms	0.91 mb
CG_3_sd.1110	50.00%	48.00%	28.00%	99	15.86 ms	163.78 ms	0.91 mb
CG_5_sd.231	58.00%	40.00%	40.00%	10	25.07 ms	172.12 ms	0.91 mb
CG_5_sd.981	58.00%	38.00%	40.00%	62	24.93 ms	171.95 ms	0.91 mb
CG_5_sd.1110	56.00%	50.00%	40.00%	91	24.81 ms	171.23 ms	0.91 mb
identity_sd.231	54.00%	40.00%	34.00%	8	0.21 ms	146.18 ms	0.54 mb
identity_sd.981	46.00%	42.00%	36.00%	95	0.22 ms	142.44 ms	0.54 mb
identity_sd.1110	50.00%	34.00%	24.00%	11	0.21 ms	143.55 ms	0.54 mb

Table A.4: MNIST - Per Layer.

Exp	Accuracy			Training Cost			
	Training	Validation	Test	Convergence Epoch	Approximation Time	Meta-Epoch Time T	Max Memory
numn_no_3_sd.231	99.39%	97.90%	98.08%	48	157.65 ms	2230.09 ms	1600.45 mb
numn_no_3_sd.981	99.37%	97.94%	98.06%	48	184.96 ms	2278.52 ms	1600.45 mb
numn_no_3_sd.523	99.45%	98.12%	98.28%	49	366.54 ms	2983.20 ms	1600.45 mb
numn_no_10_sd.231	99.29%	97.88%	98.02%	48	625.14 ms	2732.97 ms	1601.87 mb
numn_no_10_sd.981	99.30%	97.86%	98.02%	48	638.94 ms	2827.20 ms	1601.55 mb
numn_no_10_sd.523	11.24%	10.72%	10.88%	0	1266.11 ms	3863.37 ms	1600.45 mb
numn_no_20_sd.231	99.18%	97.86%	97.96%	46	1235.07 ms	3288.88 ms	1601.55 mb
numn_no_20_sd.981	99.22%	97.82%	97.94%	48	1235.14 ms	3295.44 ms	1601.87 mb
numn_no_20_sd.523	11.24%	10.72%	10.88%	0	2549.98 ms	5115.27 ms	1601.93 mb
numn_no_35_sd.231	99.00%	97.82%	97.88%	49	2162.23 ms	4238.93 ms	1601.87 mb
numn_no_35_sd.981	99.09%	97.72%	97.94%	47	2162.83 ms	4243.55 ms	1601.55 mb
numn_no_35_sd.523	11.24%	10.72%	10.88%	0	4491.73 ms	7025.65 ms	1601.87 mb
numn_no_50_sd.231	98.81%	97.68%	97.74%	48	3495.63 ms	5577.80 ms	1601.55 mb
numn_no_50_sd.981	98.85%	97.60%	97.86%	49	3590.64 ms	5648.94 ms	1601.87 mb
numn_no_50_sd.523	11.24%	10.72%	10.88%	0	6423.71 ms	8945.91 ms	1601.55 mb
CG_3_sd.231	99.43%	98.14%	98.10%	45	1214.74 ms	3512.65 ms	1428.79 mb
CG_3_sd.981	99.46%	98.02%	98.02%	48	1215.65 ms	3504.93 ms	1428.79 mb
CG_3_sd.1110	11.24%	11.24%	11.84%	0	1207.77 ms	3485.05 ms	1428.79 mb
CG_5_sd.231	99.16%	98.02%	98.10%	47	1953.80 ms	4232.78 ms	1428.79 mb
CG_5_sd.981	99.35%	98.08%	98.24%	47	1953.24 ms	4222.54 ms	1428.79 mb
CG_5_sd.1110	11.24%	11.04%	11.64%	0	1942.73 ms	4204.20 ms	1428.79 mb
CG_10_sd.231	11.24%	12.14%	10.88%	0	3615.74 ms	5877.29 ms	1428.79 mb
CG_10_sd.981	9.87%	9.22%	10.42%	1	3509.07 ms	5768.25 ms	1428.79 mb
CG_10_sd.1110	11.24%	12.14%	10.88%	0	3782.21 ms	6046.60 ms	1428.79 mb
identity_sd.231	99.44%	97.90%	98.00%	48	0.00 ms	2077.18 ms	839.03 mb
identity_sd.981	99.39%	97.98%	98.10%	49	0.00 ms	2069.42 ms	839.35 mb
identity_sd.523	99.48%	98.14%	98.20%	49	0.00 ms	2486.28 ms	839.03 mb
t1t2_sd.231	9.92%	9.70%	9.84%	0	0.00 ms	48.85 ms	165.05 mb
t1t2_sd.981	9.86%	9.40%	9.20%	0	0.00 ms	48.39 ms	165.05 mb
t1t2_sd.1110	11.24%	11.34%	11.40%	0	0.00 ms	48.39 ms	165.05 mb

Table A.5: CIFAR-10 - Per Weight (Full 1000 epochs).

Exp	Accuracy			Training Cost			
	Training	Validation	Test	Convergence Epoch	Approximation Time	Meta-Epoch Time T	Max Memory
numn_no_3_sd_231	100.00%	14.00%	14.00%	41	22.97 ms	797.21 ms	875.12 mb
numn_no_3_sd_981	100.00%	92.00%	18.00%	153	22.98 ms	796.71 ms	875.12 mb
numn_no_3_sd_1110	100.00%	96.00%	22.00%	125	22.99 ms	797.11 ms	875.12 mb
numn_no_10_sd_231	100.00%	16.00%	14.00%	14	76.66 ms	851.00 ms	875.12 mb
numn_no_10_sd_981	100.00%	12.00%	16.00%	20	76.66 ms	850.85 ms	875.12 mb
numn_no_10_sd_1110	100.00%	20.00%	16.00%	18	76.69 ms	850.93 ms	875.12 mb
numn_no_20_sd_231	100.00%	18.00%	14.00%	57	153.38 ms	926.66 ms	875.12 mb
numn_no_20_sd_981	100.00%	18.00%	20.00%	21	153.31 ms	927.02 ms	875.12 mb
numn_no_20_sd_1110	100.00%	18.00%	20.00%	262	153.43 ms	928.56 ms	875.12 mb
numn_no_35_sd_231	92.00%	12.00%	14.00%	0	268.53 ms	1043.49 ms	875.12 mb
numn_no_35_sd_981	92.00%	14.00%	16.00%	3	268.63 ms	1043.18 ms	875.12 mb
numn_no_35_sd_1110	90.00%	10.00%	14.00%	5	268.65 ms	1043.52 ms	875.12 mb
numn_no_50_sd_231	10.00%	18.00%	8.00%	2	382.64 ms	1165.06 ms	875.12 mb
numn_no_50_sd_981	10.00%	18.00%	8.00%	2	382.61 ms	1165.15 ms	875.12 mb
numn_no_50_sd_1110	10.00%	18.00%	8.00%	2	382.23 ms	1163.97 ms	875.12 mb
CG_3_sd_231	100.00%	48.00%	20.00%	117	97.14 ms	870.27 ms	1101.81 mb
CG_3_sd_981	100.00%	52.00%	16.00%	89	97.15 ms	870.02 ms	1101.81 mb
CG_3_sd_1110	100.00%	58.00%	24.00%	148	97.38 ms	870.20 ms	1101.81 mb
CG_5_sd_231	100.00%	58.00%	18.00%	169	156.90 ms	929.38 ms	1101.81 mb
CG_5_sd_981	100.00%	66.00%	18.00%	172	156.51 ms	928.91 ms	1101.81 mb
CG_5_sd_1110	100.00%	50.00%	20.00%	137	157.10 ms	929.09 ms	1101.81 mb
CG_10_sd_231	2.00%	14.00%	4.00%	1	307.22 ms	1088.98 ms	1101.81 mb
CG_10_sd_981	2.00%	14.00%	4.00%	2	307.50 ms	1090.78 ms	1101.81 mb
CG_10_sd_1110	2.00%	14.00%	4.00%	1	307.26 ms	1089.58 ms	1101.81 mb
identity_sd_231	100.00%	76.00%	22.00%	201	0.00 ms	774.13 ms	572.58 mb
identity_sd_981	100.00%	68.00%	16.00%	41	0.00 ms	774.09 ms	572.58 mb
identity_sd_1110	100.00%	72.00%	22.00%	154	0.00 ms	774.01 ms	572.58 mb
tl12_sd_231	100.00%	66.00%	22.00%	8811	0.00 ms	42.51 ms	571.97 mb
tl12_sd_981	100.00%	76.00%	22.00%	4838	0.00 ms	42.44 ms	571.97 mb
tl12_sd_1110	100.00%	72.00%	18.00%	11219	0.00 ms	42.52 ms	571.97 mb

Table A.6: CIFAR-10 - Per Weight (Early Stopping).

Exp	Accuracy			Training Cost			
	Training	Validation	Test	Convergence Epoch	Approximation Time	Meta-Epoch Time T	Max Memory
numn_no_3_sd_231	100.00%	54.00%	10.00%	41	22.88 ms	935.07 ms	875.12 mb
numn_no_3_sd_981	100.00%	100.00%	20.00%	153	22.93 ms	976.70 ms	875.12 mb
numn_no_3_sd_1110	100.00%	100.00%	26.00%	125	22.94 ms	976.61 ms	875.12 mb
numn_no_10_sd_231	98.00%	24.00%	24.00%	14	76.56 ms	945.09 ms	875.12 mb
numn_no_10_sd_981	100.00%	26.00%	18.00%	20	76.59 ms	961.41 ms	875.12 mb
numn_no_10_sd_1110	100.00%	24.00%	18.00%	18	76.57 ms	961.68 ms	875.12 mb
numn_no_20_sd_231	100.00%	22.00%	16.00%	57	153.18 ms	1005.33 ms	875.12 mb
numn_no_20_sd_981	98.00%	30.00%	26.00%	21	153.20 ms	1048.09 ms	875.12 mb
numn_no_20_sd_1110	98.00%	14.00%	10.00%	19	153.19 ms	1017.74 ms	875.12 mb
numn_no_35_sd_231	88.00%	14.00%	14.00%	0	267.96 ms	1133.01 ms	875.12 mb
numn_no_35_sd_981	90.00%	12.00%	16.00%	3	267.96 ms	1132.94 ms	875.12 mb
numn_no_35_sd_1110	88.00%	12.00%	12.00%	5	267.96 ms	1133.05 ms	875.12 mb
numn_no_50_sd_231	10.00%	18.00%	8.00%	2	381.70 ms	1364.58 ms	875.12 mb
numn_no_50_sd_981	10.00%	18.00%	8.00%	2	383.59 ms	2933.08 ms	875.12 mb
numn_no_50_sd_1110	10.00%	18.00%	8.00%	2	384.22 ms	3046.32 ms	875.12 mb
CG_3_sd_231	100.00%	84.00%	26.00%	136	97.30 ms	1032.90 ms	1101.81 mb
CG_3_sd_981	100.00%	82.00%	22.00%	38	97.18 ms	1014.32 ms	1101.81 mb
CG_3_sd_1110	100.00%	82.00%	22.00%	22	97.31 ms	1008.32 ms	1101.81 mb
CG_5_sd_231	100.00%	36.00%	24.00%	7	156.82 ms	991.17 ms	1101.81 mb
CG_5_sd_981	100.00%	94.00%	24.00%	177	157.72 ms	1034.26 ms	1101.81 mb
CG_5_sd_1110	100.00%	92.00%	26.00%	127	157.46 ms	1045.05 ms	1101.81 mb
CG_10_sd_231	12.00%	12.00%	10.00%	0	307.33 ms	1250.11 ms	1101.81 mb
CG_10_sd_981	12.00%	12.00%	10.00%	0	308.25 ms	2274.14 ms	1101.81 mb
CG_10_sd_1110	12.00%	12.00%	10.00%	0	309.70 ms	3052.81 ms	1101.81 mb
identity_sd_231	100.00%	86.00%	22.00%	75	0.00 ms	912.48 ms	572.58 mb
identity_sd_981	100.00%	76.00%	20.00%	41	0.00 ms	900.30 ms	572.58 mb
identity_sd_1110	100.00%	80.00%	22.00%	100	0.00 ms	2162.10 ms	572.58 mb

Table A.7: CIFAR-10 - Per Layer.

Exp	Accuracy			Training Cost			
	Training	Validation	Test	Convergence Epoch	Approximation Time	Meta-Epoch Time T	Max Memory
numn_no_3_sd_231	98.67%	55.58%	55.08%	28	3101.19 ms	12984.61 ms	5601.64 mb
numn_no_3_sd_981	98.93%	55.66%	55.10%	25	3100.71 ms	12995.64 ms	5601.64 mb
numn_no_3_sd_1110	98.32%	55.64%	55.18%	38	3101.03 ms	12994.88 ms	5601.64 mb
numn_no_10_sd_231	31.41%	32.08%	30.50%	43	10356.82 ms	20225.30 ms	5601.64 mb
numn_no_10_sd_981	31.54%	32.00%	31.06%	5	10352.13 ms	20243.04 ms	5601.64 mb
numn_no_10_sd_1110	41.10%	41.26%	40.82%	48	10360.92 ms	20293.44 ms	5601.64 mb
numn_no_20_sd_231	27.55%	28.84%	23.32%	2	20758.27 ms	30623.70 ms	5601.64 mb
numn_no_20_sd_981	30.98%	31.72%	30.42%	5	20737.55 ms	30662.66 ms	5601.64 mb
numn_no_20_sd_1110	33.86%	33.92%	31.44%	9	20743.40 ms	30628.73 ms	5601.64 mb
numn_no_35_sd_231	29.93%	30.82%	22.98%	43	36252.12 ms	46182.87 ms	5601.64 mb
numn_no_35_sd_981	27.93%	29.24%	23.06%	4	36254.22 ms	46170.08 ms	5601.64 mb
numn_no_35_sd_1110	27.83%	29.24%	24.20%	3	36358.74 ms	46240.10 ms	5601.64 mb
numn_no_50_sd_231	25.34%	26.70%	23.22%	3	51963.54 ms	61859.36 ms	5601.64 mb
numn_no_50_sd_981	27.78%	28.76%	23.30%	4	51729.27 ms	61616.66 ms	5601.64 mb
numn_no_50_sd_1110	30.53%	31.06%	25.12%	5	51956.86 ms	61910.07 ms	5601.64 mb
CG_3_sd_231	98.96%	56.80%	54.08%	28	9654.95 ms	18798.29 ms	5214.49 mb
CG_3_sd_981	98.43%	56.30%	55.26%	37	9658.85 ms	18804.82 ms	5214.49 mb
CG_3_sd_1110	98.91%	56.10%	55.16%	44	9644.06 ms	18761.14 ms	5214.49 mb
CG_5_sd_231	34.84%	35.92%	34.76%	49	15442.94 ms	24572.34 ms	5214.49 mb
CG_5_sd_981	40.69%	41.42%	39.80%	46	15435.95 ms	24561.46 ms	5214.49 mb
CG_5_sd_1110	31.23%	31.60%	10.32%	2	13863.82 ms	22843.40 ms	5214.49 mb
CG_10_sd_231	16.76%	16.58%	10.16%	0	26809.23 ms	35739.90 ms	5214.49 mb
CG_10_sd_981	17.21%	16.90%	10.16%	0	26880.70 ms	35814.25 ms	5214.49 mb
CG_10_sd_1110	21.52%	22.22%	10.16%	1	26843.49 ms	35799.44 ms	5214.49 mb
identity_sd_231	98.19%	55.74%	53.92%	37	0.00 ms	9931.71 ms	3029.88 mb
identity_sd_981	99.13%	55.88%	55.88%	49	0.00 ms	9870.14 ms	3029.88 mb
identity_sd_1110	98.45%	55.44%	55.26%	39	0.00 ms	9767.52 ms	3029.88 mb
t1t2_sd_231	99.93%	56.34%	55.34%	9461	0.00 ms	321.14 ms	2415.42 mb
t1t2_sd_981	99.89%	56.18%	54.70%	22069	0.00 ms	321.19 ms	2415.42 mb
t1t2_sd_1110	99.91%	56.70%	56.08%	14109	0.00 ms	321.15 ms	2415.42 mb

A.2 Baselines Regularization Results

Table A.8: Baseline results for various regularization weights for an MLP with as many hidden neurons as inputs.

L_2 Weight	Accuracy		
	Training	Validation	Test
CIFAR-10			
1×10^{-6}	58.29±0.24%	51.60±0.20%	50.39±0.54%
1×10^{-5}	58.32±0.24%	51.64±0.21%	50.41±0.69%
1×10^{-4}	58.17±0.20%	51.54±0.23%	50.39±0.56%
1×10^{-3}	57.57±0.21%	51.39±0.21%	50.09±0.76%
1×10^{-2}	53.09±0.30%	49.70±0.31%	47.81±0.43%
1×10^{-1}	42.29±0.23%	42.31±0.49%	40.82±0.88%
5×10^{-1}	34.48±0.18%	34.94±0.18%	29.93±0.48%
1	31.06±0.46%	31.64±0.31%	22.43±0.34%
2	28.24±0.40%	28.67±0.26%	15.55±0.43%
3	26.28±0.83%	26.52±0.53%	10.05±0.06%
MNIST			
1×10^{-6}	94.78±0.10%	94.81±0.25%	94.41±0.14%
1×10^{-5}	94.78±0.09%	94.82±0.24%	94.41±0.14%
1×10^{-4}	94.78±0.09%	94.82±0.25%	94.43±0.12%
1×10^{-3}	94.73±0.10%	94.81±0.23%	94.39±0.17%
1×10^{-2}	93.99±0.10%	94.28±0.26%	93.67±0.09%
1×10^{-1}	89.89±0.06%	90.72±0.10%	89.93±0.21%
5×10^{-1}	82.24±0.30%	83.48±0.13%	80.39±0.52%
1	74.26±0.25%	75.80±0.28%	55.37±1.56%
2	67.67±2.16%	69.13±1.64%	15.57±3.35%
3	57.75±3.88%	59.15±3.36%	11.17±0.15%

A.3 Training Evolution Plots for Main Experiments

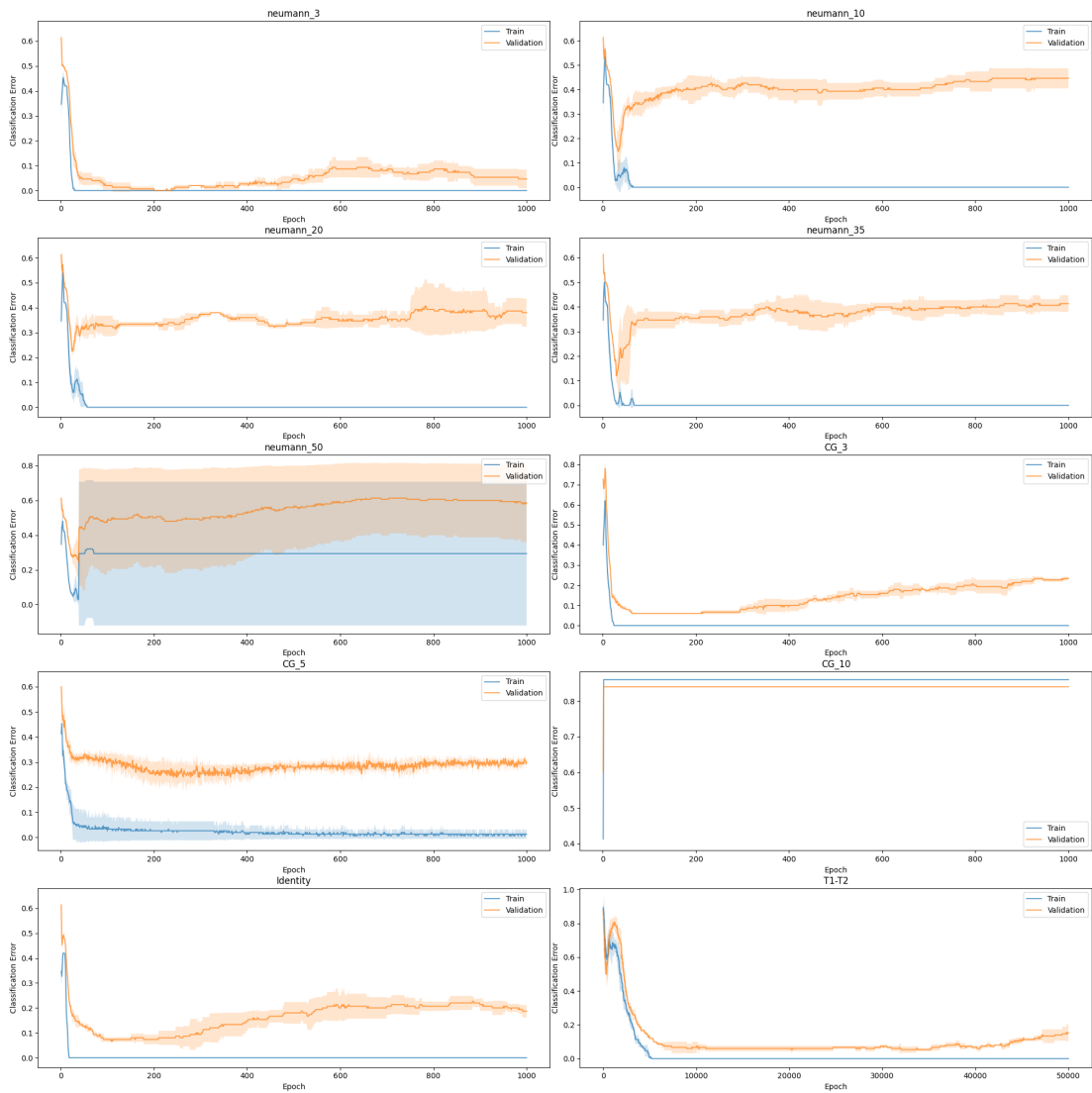


Figure A.1: Training Metrics Evolution for MNIST Overfitting a Small Validation Set Experiments.

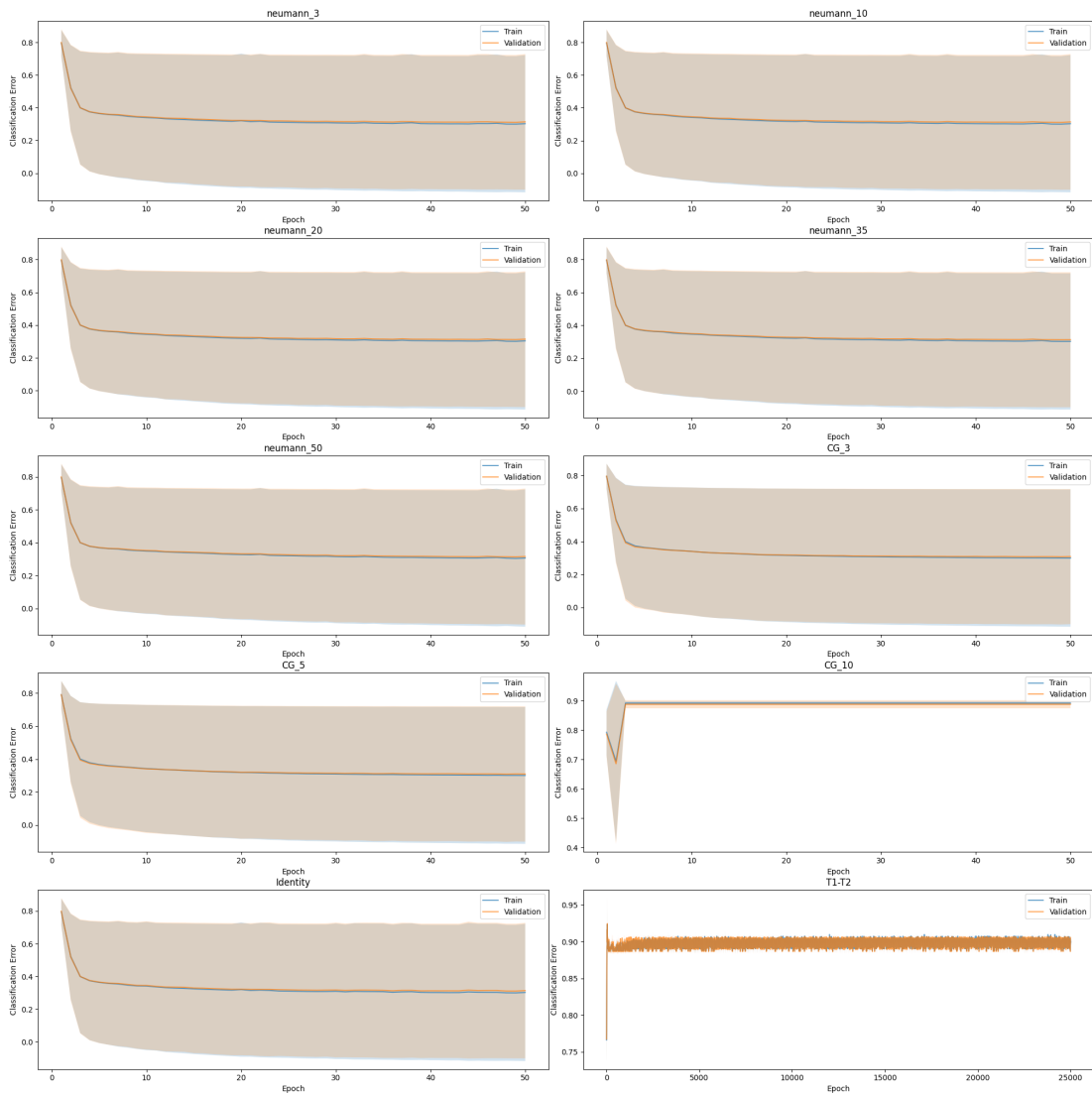


Figure A.2: Training Metrics Evolution for MNIST Learning Per Layer L_2 Regularization Weight Experiments. Note the extreme high variance and bad performance of most methods here. This is a result of including bad seeds whose training was unstable. As stated, the results in the main body of the report only included stable seeds since finding working seeds was challenging.

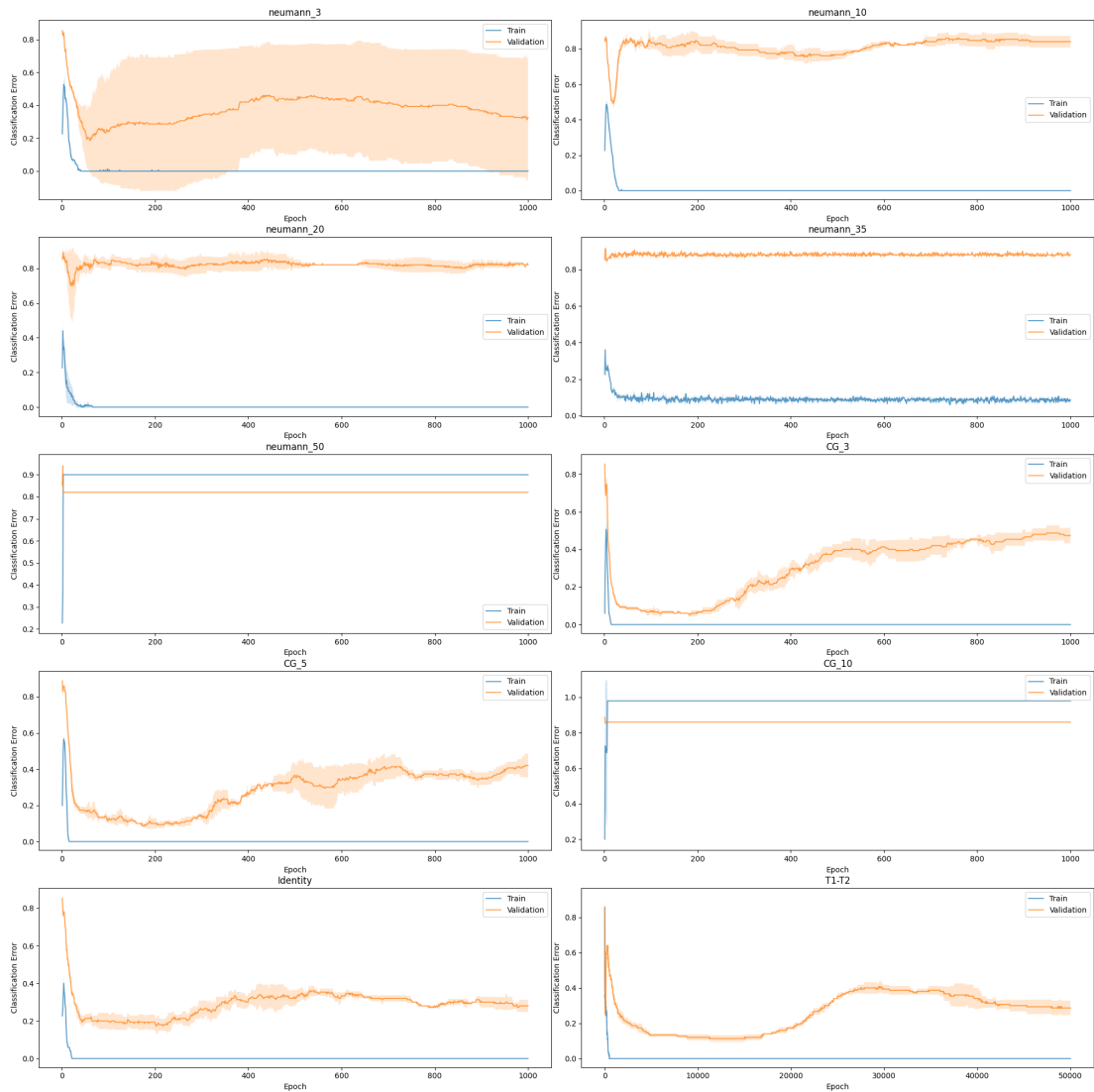


Figure A.3: Training Metrics Evolution for CIFAR-10 Overfitting a Small Validation Set Experiments.

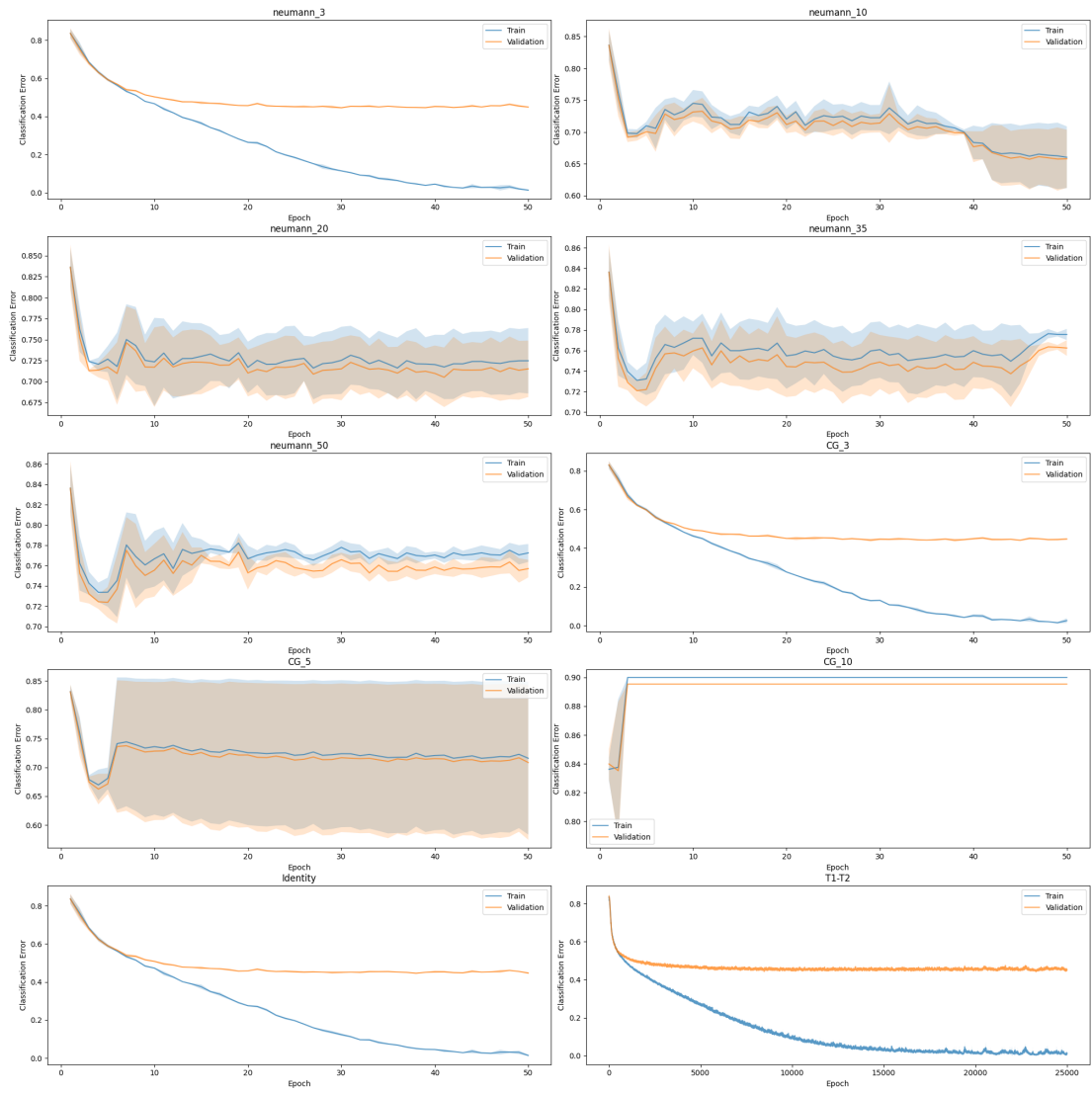


Figure A.4: Training Metrics Evolution for CIFAR-10 Learning Per Layer L_2 Regularization Weight Experiments.

Appendix B

Ablation Study Training Evolution Plots

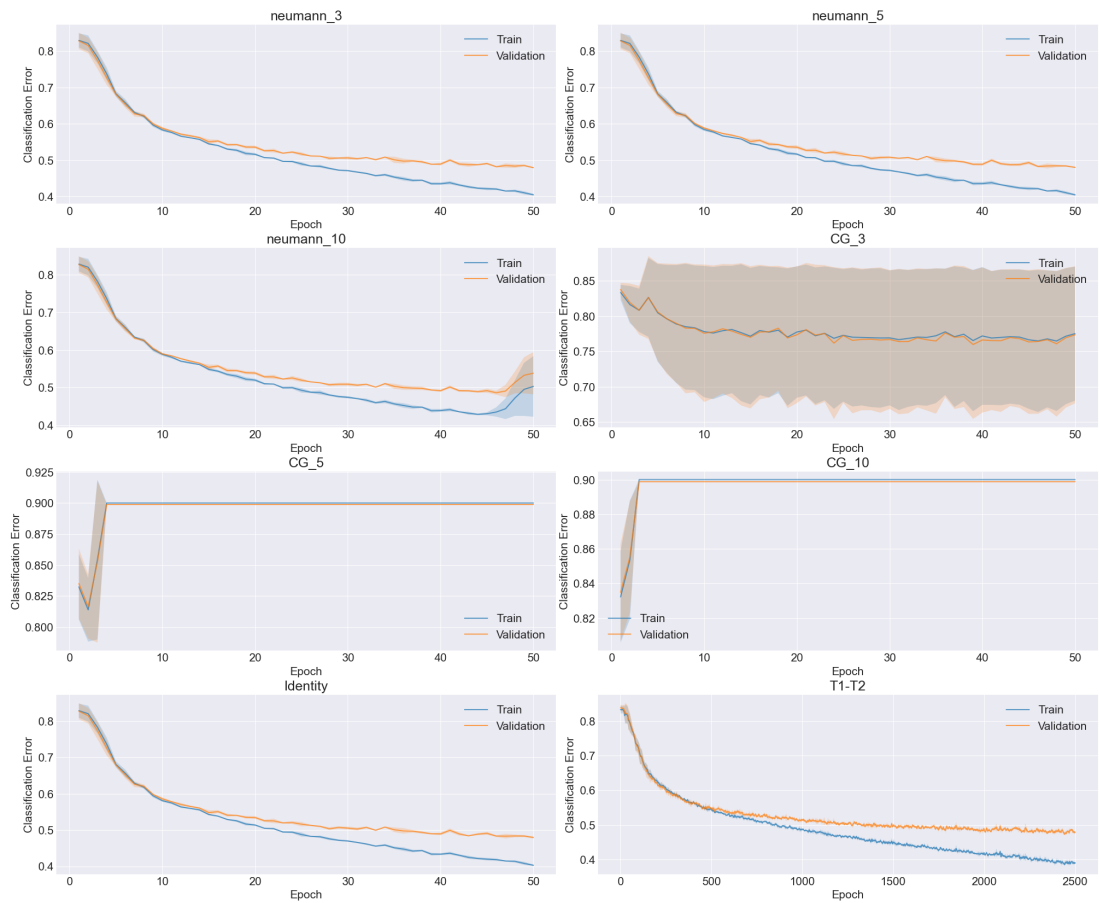


Figure B.1: Training Metrics Evolution for Ablation Study, section 4.2.4, when using 50 inner loop steps.

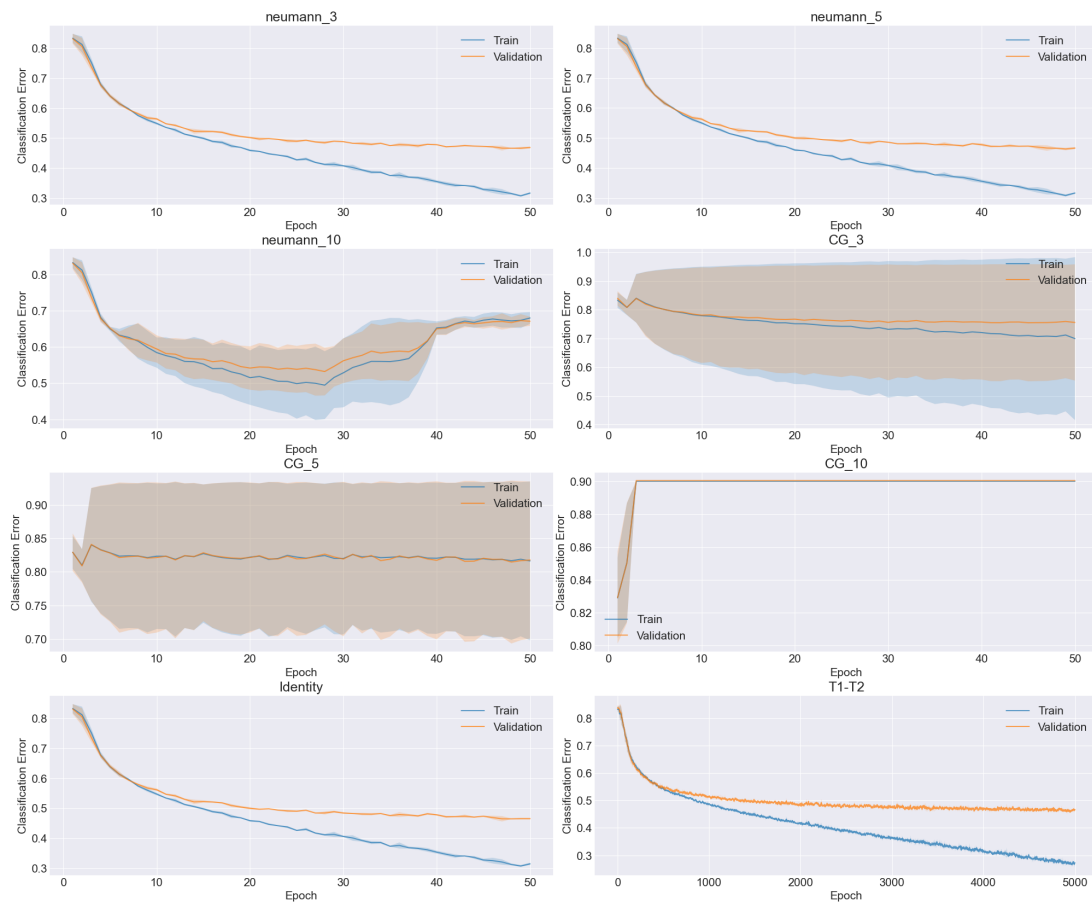


Figure B.2: Training Metrics Evolution for Ablation Study, section 4.2.4, when using 100 inner loop steps.

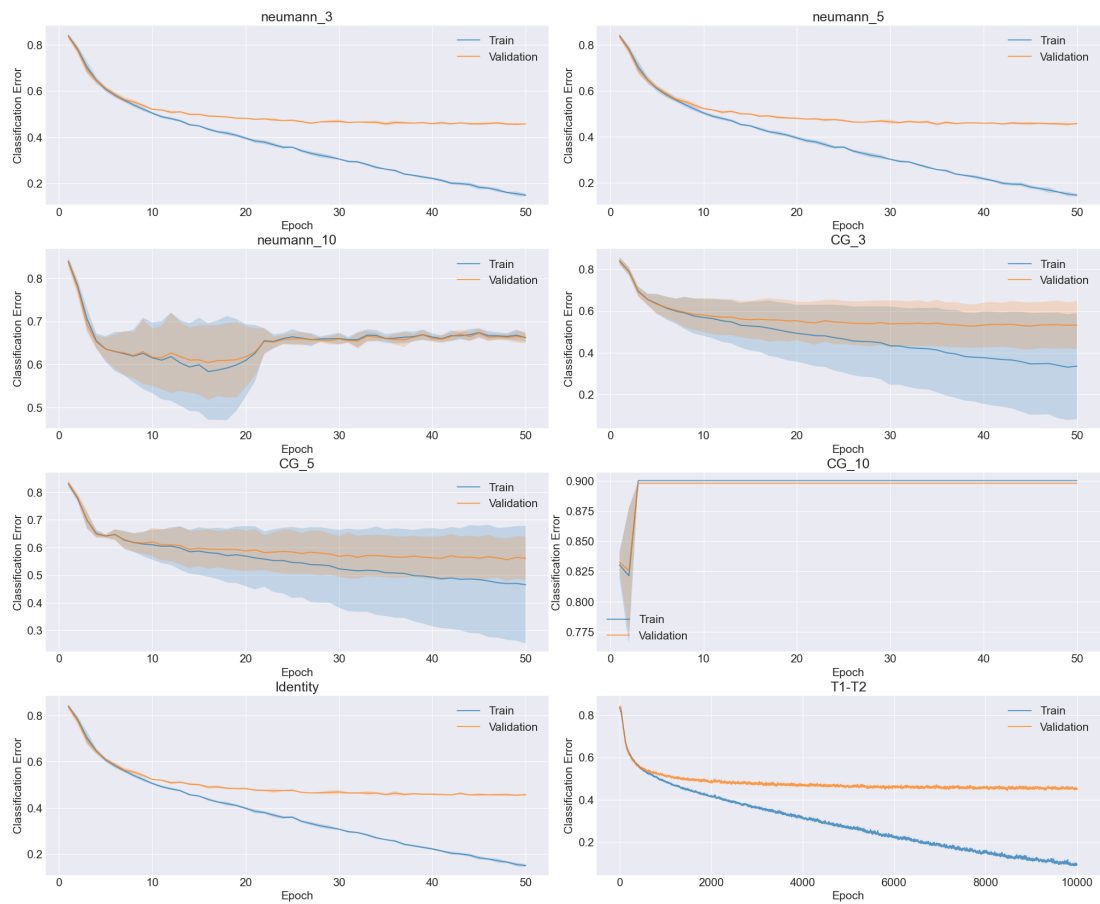


Figure B.3: Training Metrics Evolution for Ablation Study, section 4.2.4, when using 200 inner loop steps.

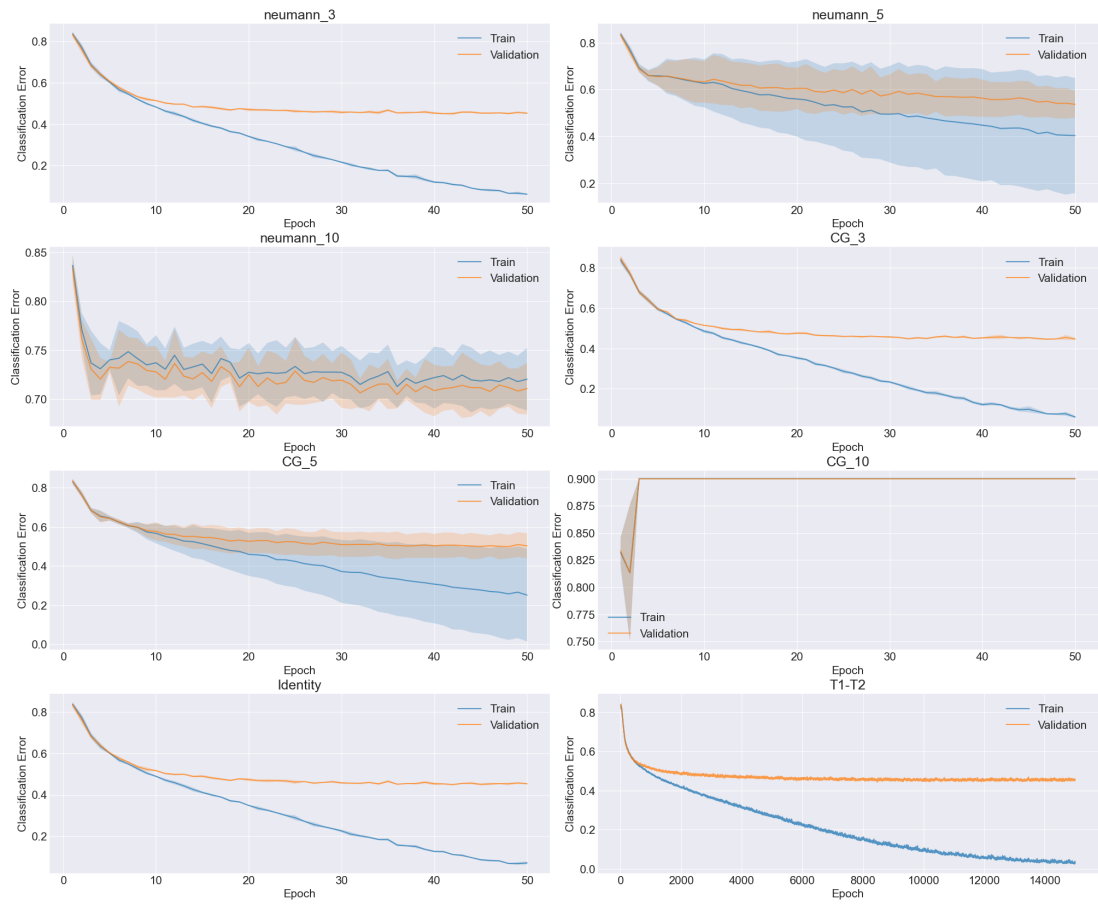


Figure B.4: Training Metrics Evolution for Ablation Study, section 4.2.4, when using 300 inner loop steps.

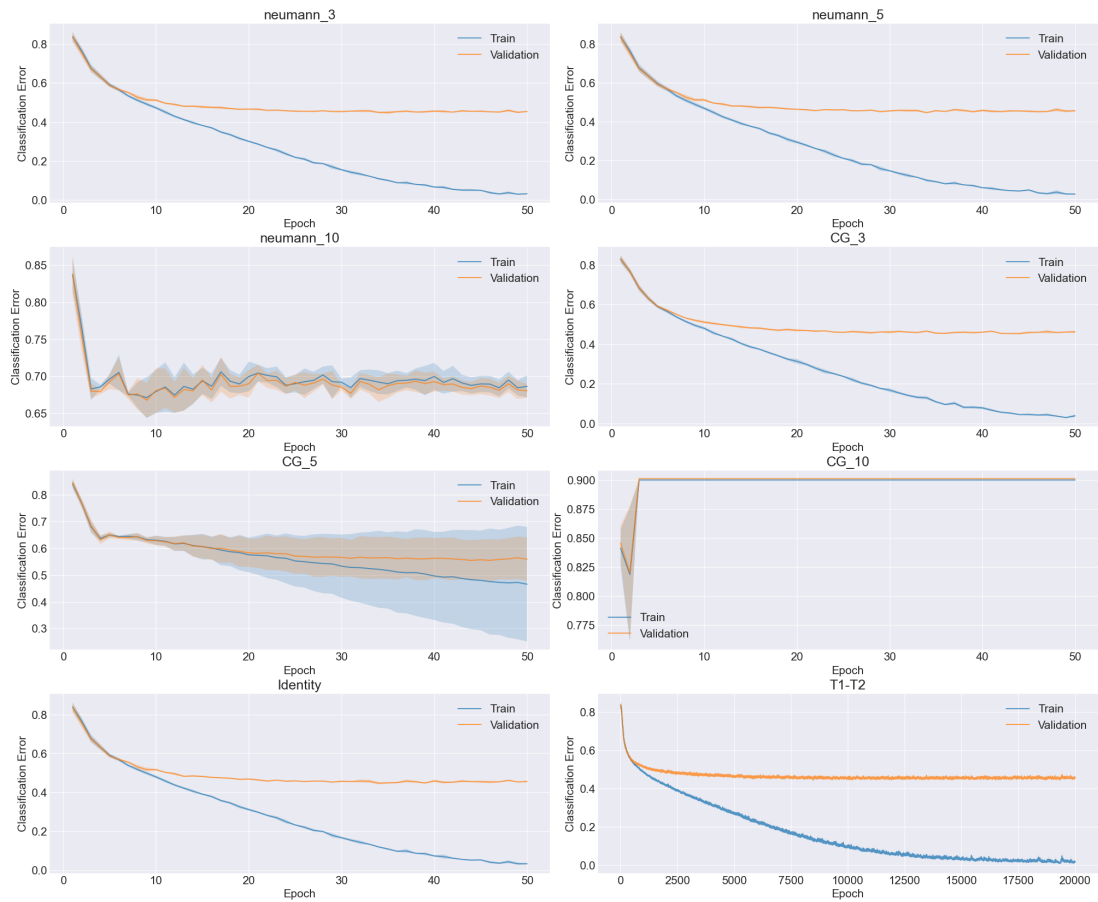


Figure B.5: Training Metrics Evolution for Ablation Study, section 4.2.4, when using 400 inner loop steps.

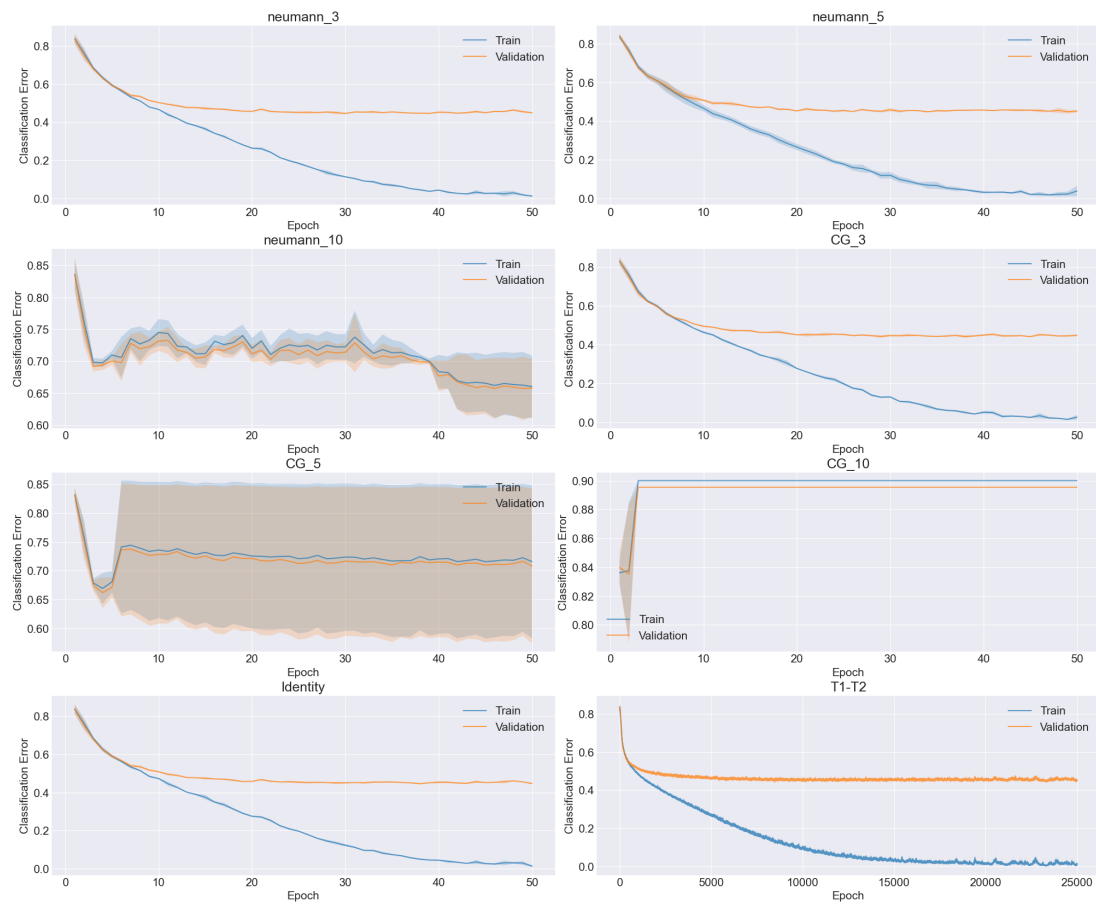


Figure B.6: Training Metrics Evolution for Ablation Study, section 4.2.4, when using 500 inner loop steps.